**Myocardin-dependent Kv1.5 channel expression prevents phenotypic modulation of human vessels in organ culture.**

Marycarmen Arévalo-Martínez[1,2], Pilar Cidad[1,2], Nadia García-Mateo[1,2], Sara Moreno-Estar[1,2], Julia Serna[1,2], Mirella Fernández[5], Karl Swärd[6], María Simarro[3,2], Miguel A de la Fuente[4,2], José R López-López[1,2,] * and M Teresa Pérez-García[1,2,] *.

**Short title**: Kv1.3/Kv1.5 ratio governs human vessel remodeling

**Afiliations:** [1]Departamento de Bioquímica y Biología Molecular y Fisiología, [3]Departamento de Enfermería, [4]Departamento de Biología Celular, Universidad de Valladolid, [2]Instituto de Biología y Genética Molecular (IBGM), CSIC, [5]Cardiovascular Surgery Department, Hospital Clínico Universitario de Valladolid, Spain, [6]Department of Experimental Medical Science, University of Lund, Sweden.

**Correspondence:**

Dr M. Teresa Pérez García
Departamento de Bioquímica y Biología Molecular y Fisiología
Universidad de Valladolid
Edificio IBGM, c/ Sanz y Forés, 3
47003 Valladolid, SPAIN
tperez@ibgm.uva.es

*equal senior authors

**Word count**: 8943

**Subject codes:** Vascular Biology, Restenosis, Smooth Muscle Proliferation and Differentiation, Ion Channels/Membrane Transport

**TOC category:** Basic. **TOC subcategory:** Vascular Biology

**ABSTRACT**

**Objective:** We have previously described that changes in the expression of Kv channels associate to phenotypic modulation (PM), so that Kv1.3 /Kv1.5 ratio is a landmark of vascular smooth muscle cells (VSMCs) phenotype. Moreover, we demonstrated that the Kv1.3 functional expression is relevant for PM in several types of vascular lesions. Here, we explore the efficacy of Kv1.3 inhibition for the prevention of remodeling in human vessels, and the mechanisms linking the switch in Kv1.3 /Kv1.5 ratio to PM.

**Approach and Results:** Vascular remodeling was explored using organ culture and primary cultures of VSMCs obtained from human vessels. We studied the effects of Kv1.3 inhibition on serum-induced remodeling, as well as the impact of viral vector-mediated overexpression of Kv channels or myocardin knock-down. Kv1.3 blockade prevented remodeling by inhibiting proliferation, migration and extracellular matrix (ECM) secretion. PM activated Kv1.3 via downregulation of Kv1.5. Hence, both Kv1.3 blockers and Kv1.5 overexpression inhibited remodeling in a non-additive fashion. Finally, myocardin knock-down induced vessel remodeling and Kv1.5 downregulation and myocardin overexpression increased Kv1.5, while Kv1.5 overexpression inhibited PM without changing myocardin expression.

**Conclusions:** We demonstrate that Kv1.5 channel gene is a myocardin-regulated, VSMCs contractile marker. Kv1.5 downregulation upon PM leaves Kv1.3 as the dominant Kv1 channel expressed in dedifferentiated cells. We demonstrated that the inhibition of Kv1.3 channel function with selective blockers or by preventing Kv1.5 downregulation can represent an effective, novel strategy for the prevention of intimal hyperplasia and restenosis of the human vessels used for coronary angioplasty procedures.

**Key Words: Kv1 channels, phenotypic modulation, vascular smooth muscle, remodeling**

**Non-standard Abbreviations and Acronyms**

PM: Phenotypic modulation
hMA: human mammary artery
hSV: human saphenous vein
VSMCs: Vascular smooth muscle cells
PAP-1: 5-(4-phenoxybutoxy) psoralen
MgTx: Margatoxin
SM22: Smooth Muscle 22-alpha gene, Transgelin
αSMA: Alpha-smooth muscle actin
MHCII: Myosin heavy chain II
ccMYOCD: Knock-down of myocardin by using a CRISPR-Cas9 strategy
Lv: Lentiviral vector
AAV: Adeno-Associated viral vector

## INTRODUCTION

VSMCs in the vessel wall are able to switch from a contractile, quiescent state to a synthetic phenotype, characterized by migration, proliferation, loss of contractile proteins and enhanced synthesis of ECM components [1]. This PM is necessary for vessel growth and repair, but it also contributes to the pathogenesis of atherosclerosis, vein graft adaptation, transplant arteriopathy, and restenosis after percutaneous transluminal coronary angioplasty. Vascular injury of any kind results in a stereotypical healing response culminating in intimal VSMC recruitment and activation, leading to intimal hyperplasia. PM is central to this process, which determines the progressive stiffening of the vessel wall and the narrowing of the vessel lumen. Despite significant advances in vascular biology, bioengineering, and pharmacology, restenosis remains the Achilles heel of percutaneous and open vascular procedures. To date, therapies directed to prevent restenosis include drug-eluting stents comprising a polymer-based delivery of either inhibitors of the mammalian target of rapamycin (mTOR) or the antimitotic agent paclitaxel. These are potent antiproliferative agents which also have additional effects on ECM synthesis. However, as they are not specific for VSMCs, an increased incidence of late in-stent thrombosis, due to delayed reendothelialization has been reported [2].

Despite the substantial interest in the search for novel anti-restenosis therapies, the mechanisms of VSMC PM are incompletely understood. PM is controlled by many transcriptional regulatory pathways, in particular serum response factor (SRF) and its cofactor, myocardin [3,4]. Some other repressor pathways such as Krupple-like factor-4/5 (KLF4/5), ETS-like transcription factor-1 (Elk-1), HES-related repressor protein-1 (Herp1), FoxO4, and the p65 subunit of NFκB, have also been suggested to act as molecular switches regulating VSMC differentiation (reviewed in [1,5]). These mechanisms are not mutually exclusive, and combinations of these factors modulate PM through both myocardin-dependent and independent pathways.

However, many candidates acting on some of these pathways have proven unsuccessful in preventing intimal hyperplasia in spite of being specific to their targets in *in vitro* studies and even effective in animal models, as was the case for the platelet inhibitor abciximab or the calcium channel blockers[6–8] . Species and/or vascular bed specific processes may lie behind these discrepancies. Moreover, the use of healthy, large, peripheral vessels in mice to model the response of small (coronary) diseased vessels constitutes an important limitation. Restenosis will occur in pathological vessels and the underlying disease determines prognosis, evidencing the need of testing these novel modulators in the same vessels that can undergo vascular surgery. Previous work from several groups has shown that blockade of the voltage-dependent potassium channel Kv1.3 can represent a specific, VSMCs phenotype-dependent antiproliferative therapy[9,10]. Using an expression profile of ion channel genes in VSMCs from mouse femoral arteries, we showed that Kv1.3 currents were upregulated in proliferating VSMCs and that their selective blockade inhibited migration and proliferation [9]. In addition, in vivo proliferative lesions in a model of endovascular injury were significantly reduced by systemic infusion of Kv1.3 blockers [11]. Of interest, the increased contribution of Kv1.3 channels upon PM associates with a marked decreased expression of Kv1.5 channels. In fact, changes in Kv1.3/Kv1.5 ratio are a

conserved landmark of PM, as they have been found in all vascular beds examined, including human samples [12,13]. In native, quiescent VSMCs, Kv1.5 is the dominant Kv1 channel expressed, most likely forming heteromultimeric Kv1 channels [14], but in proliferating VSMCs, Kv1 currents are almost exclusively mediated through Kv1.3 channels. Upon heterologous expression, Kv1.5 channels decreased proliferation while Kv1.3 channels increased it. Moreover, the effects on proliferation of Kv1.3/Kv1.5 chimeras and mutant channels pinpoint key residues within the C-terminus that determine Kv1.3-induced proliferation [15]. Based on these previous observations, we hypothesize that the dominant expression of Kv1.5 in Kv1 heterotetramers in contractile VSMC interfere with the accessibility of key docking sites at the C-terminus of Kv1.3 channels, thus inhibiting Kv1.3 induced-proliferation. Upon PM, the loss of Kv1.5 channels allows Kv1.3 voltage-induced conformational changes leading to activation of proliferative pathways.

Here, we have explored the efficacy of Kv1.3 channel blockade for the prevention of intimal hyperplasia in human vessels and the mechanisms linking the Kv1.5 to Kv1.3 switch to PM. Using human saphenous veins (hSV) and internal mammary arteries (hMA) from patients undergoing coronary bypass surgery we obtained vessel rings for organ culture experiments and primary VSMCs cultures. In these two preparations we have explored the effects of Kv1.3 blockade on the matrix synthesis or proliferative, and migratory responses induced by serum or PDGF stimulation. Genetic manipulation of Kv1.3 and Kv1.5 was used both in cell and organ culture to study the effect of these two channels on PM of VSMCs. Our data indicate that Kv1.5 is a contractile marker, whose expression levels are positively regulated by myocardin expression, so that PM can be prevented when overexpressing Kv1.5 channels, by a mechanism that involves competition with Kv1.3 channels.

## MATERIALS AND METHODS

The data that support the findings of this study are available from the corresponding author upon reasonable request.

***Samples.*** hMA and hSV belonging to the COLMAH collection were obtained from donors undergoing bypass surgery at the Clinic Hospital of Valladolid, with procedures approved by the Hospital Ethics Committee and according to the Helsinki Declaration. The vessels were collected in culture medium and used in the next 24 hours for organ culture, primary VSMCs culture or RNA and protein extraction.

***Organ culture and primary culture of human VSMCs.*** For organ culture experiments, hMA and hSV were cut in 5mm rings, placed in MEM culture medium (Gibco) supplemented with penicillin-streptomycin (100U/ml each), 5µg/ml Fungizone and 2mM L-glutamine and kept for 2 weeks at 37ºC in 5% CO2 humidified atmosphere. 20% Fetal Bovine Serum (FBS) was added to induce intimal hyperplasia (positive control), while FBS-free medium was used as negative control. Experimental conditions include the addition of the Kv1.3 blockers 5-(4-phenoxybutoxy) psoralen (PAP-1) or Margatoxin (MgTx) or other drugs as indicated to the 20%FBS medium. In all cases sequential sections of the same artery were used for the different experimental conditions.

Primary VSMCs culture were obtained from explants of human vessels after removal of endothelial and adventitia layers as described elsewhere [12]. Cells in passages 3-9 were used for proliferation, migration and electrophysiological studies. The smooth muscle origin of the cells was supported by their labelling with smooth muscle-specific antibodies such as α-smooth muscle actin (αSMA, Supplemental figure I).

***Histology and immunohistochemistry.*** hMA and hSV rings were embedded in paraffin to obtain 7µm-thick sections as described elsewhere [16]. Morphometric analysis was performed with Masson trichrome stained sections, sequentially treated with iron hematoxylin (30 min), Biebrich scarlet acid fuchsin (20 min) and Light Green (3 min) and analyzed using computerized morphometry (ImageJ). Measures included luminal, intimal, media and vessel area. From these, the intima to media ratio (I/M ratio) and percentage of stenosis were calculated [16]. For analysis of nuclei number, sections were incubated with Hoechst at 1:2000 for 30 minutes. Elastin abundance was quantified by measuring elastin auto-fluorescence. DAB immunohistochemistry was done as previously described [9]. Primary antibodies against Kv1.5, myocardin, SM22, MHCII and GFP (see the Major Resources Table in the Supplemental Material) were used at 1:50-1:200 concentration. Secondary antibodies goat anti-Rabbit HRP (Dako) and goat anti-Mouse HRP (DAKO) were used at 1:1000 concentration.

***RNA isolation and Real time PCR.*** RNA was extracted from arterial rings or cultured VSMCs with TRIzol Reagent following the manufacturer´s instructions, and real-time qPCR was performed as detailed elsewhere [12]. mRNA levels were determined with Taqman™ assays (ThermoFisher ) in a Rotor-Gene 3000 instrument. The relative abundance quantification method ($2^{-\Delta CT}$) was used to determine mRNA levels of Kv1.3, Kv1.5, Calponin, Myocardin, Kvβ2, GFP and the alpha1 subunits of collagen I, III and VIII, with ribosomal protein L18 (RPL18) as the housekeeping gene (see the Major

Resources Table in the Supplemental Material). RNA extraction from formalin-fixed paraffin-embedded tissue was described elsewhere [17]. For the Myocardin and MRTF-A and MRTF-B transduced cells, ribosomal protein 18S was the housekeeping gene, null virus transduced cells were used as control and a Ct=40 was assigned in cases the expression was not detected.

***Viral vector construction and infections.*** Plasmids expressing the full-length Kv1.5-EGFP, Kv1.3-Cherry, mutant WF-Kv1.3-EGFP and mutant Y2-Kv1.3-Cherry have been previously described [12,15]. Control plasmids coding for EGFP or Cherry inserts alone were used as a control. All inserts of the above plasmids were digested with the appropriate restriction enzymes and further subcloned into the adeno-associated viral (AAV) vector pAAV-MCS. Viral particles were produced using the AAV Helper-Free System (Agilent Technologies) according to manufacturer's instructions. Virus titration was done by qPCR with the primers targeting the ITRs regions: FW-ITR primer: 5´-GGAACCCCTAGTGATGGAGTT-3´ and REV-ITR primer: 5´-CGGCCTCAGTGAGCGA-3´ [18].

For AAV transduction of primary VSMC cultures, 60 µl of $10^{10}$ viral particles/mL (≈500 particles/cell) were added to 80% confluent VSMC and incubated during 4h in Optimem medium (Invitrogen), following by 48h incubation in complete media. Afterwards, cells were used for proliferation, migration and electrophysiological studies for 3 passages at most. Efficiency of transduction was monitored by the expression of the reporter protein and was routinely over 80-90%.

EGFP, Kv1.5-EGFP and Kv1.3-Cherry were also cloned into the lentiviral vector pSin-EF2-Sox2-Pur (a gift from James Thomson, Addgene plasmid #16577), digested with EcoRI and SpeI. Lentiviral stocks were produced by transient cotransfection into the human 293FT cell line (Thermo Fisher Scientific) as described elsewhere [19]. Stock Virus titers were between $10^6$-$10^8$ particles/ml. VSMCs cells were transduced with a MOI of 30-50 viral particles/cell in Optimen with 5µg/ml protamine and selected with 2 µg/ml puromycin for at least 5 days before assaying.

Transduction of human coronary VSMCs (hCASMCs) was carried out using commercial adenoviral vectors (100 MOI: null (#1300), MYOCD (ADV-216227), MRTF-A (ADV-215499), MRTF-B (ADV-215500); all from Vector Biolabs). hCASMCs were cultured and transduced as described [20,21].

For the construction of the myocardin knock-down (ccMYOCD), we used the lentiCRISPR v2 plasmid, expressing a single sgRNA under the hU6 promoter and the WT Cas9 nuclease under the EFS promoter (a gift from Feng Zhang, Addgene plasmid #52961). We modified this vector replacing the unique hU6-sgRNA cloning site cassette with an insert containing two sgRNAs cloning sites under independent U6 promoters. Target sequences in myocardin exons 1 (with 5' overhang BsmBI digestion sites) and 10 (with 5' overhang BsaI digestion sites) were selected with the software tool CRISPOR [22] (see sequences in the Major Resources Table in the Supplemental Material), and the scores obtained are shown in Supplemental Table I. The lentiCRISPR v2 plasmid, expressing a single sgRNA was also used to create two other Myocardin knockdown vectors, targeting only exon 1 (CRISPR-1) or exon 10 (CRISPR-10), as controls for off target effects of ccMYOCD. The oligos were annealed and inserted sequentially into

the lentiCRISPR v2 backbone. sgRNA sequences and plasmids were confirmed by Sanger sequencing.

When infecting vessel in organ culture, viral incubation in Optimen lasted for 96 h in the presence of protamine (10µg/ml). Arterial rings were kept in culture medium with the indicated treatments for two weeks.

***Electrophysiological methods***. Ionic currents were recorded at room temperature (20-25ºC) using the whole-cell configuration of the patch-clamp technique. Whole-cell current recordings and data acquisition from cultured VSMC cells were made as previously described [13,23]. VSMCs were perfused with a solution containing (in mM): 141 NaCl, 4.7 KCl, 1.2 MgCl2, 1.8 CaCl2, 10 glucose, 10 HEPES, pH 7.4 (with NaOH). 0.5 µM Paxilline was included in the bath solution to block large conductance $Ca^{2+}$-dependent $K^+$ channels. Patch pipettes were filled with a solution containing (in mM): 125 KCl, 4 MgCl2, 10 HEPES, 10 EGTA, 5 MgATP; pH 7.2 with KOH. Current/voltage curves were constructed from potentials ranging from -60 to +100mV in 10 mV steps. Kv1.3 and Kv1.5 components were defined as the PAP-1 (100 nM) or diphenyl-iodinium (DPO, 100nM) sensitive currents.

***Proliferation assays***. The percentage of cells at the S phase was quantified using EdU (5-ethynyl-2´-deoxyuridine) incorporation for 6h with a commercial kit (Click-iT® EdU Imaging Cell Proliferation Assay, Invitrogen) as described [13]. Briefly, 25,000 VSMCs were seeded onto poly-l-lysine coated coverslips placed in 12 mm wells with control media (10% FBS). Next day, media was replaced with serum-free (SF) media, and proliferation was induced by addition of PDGF (20 ng/ml), alone or in combination with the indicated blockers during 24 h. Determinations were carried out in triplicate samples and controls were included in all experiments.

***Migration assays*** Scratch assays were performed as described [9]. Monolayers of confluent VSMCs were scraped with a 10 µl pipette tip and incubated in 0.5 % FBS medium alone or with 100nM PAP-1. Pictures were taken at 0, 4, 8, 12 and 24 hours from scratch and the percentage of invaded area was determined using ImageJ software. For Boyden chamber assay 20,000 VSMCs were seeded in polycarbonate inserts placed in 24 well plates (Nunc™, 140629). The well was filled with 500 µl of culture medium (0% or 20% FBS) and the number of migrated cells after 18h was determined as described [24] using ImageJ.

***Statistical analysis.*** Statistical Analysis was performed using Microsoft Excel and R studio software packages. Pooled data are expressed as means ±SEM and differences were considered statistically significant when $p < 0.05$. Shapiro-Wilk test and Bartlett's test were used to test normality and homogeneity of variances respectively. For pairwise comparison of normal distributions, Student's t test was used, otherwise Mann-Whitney U test was applied. For comparisons among several groups, one-way ANOVA followed by Tukey's test was employed in the case of normal distributions and equal variances, and Kruskal-Wallis analysis followed by Dunn's test was applied. Linear correlation between variables was measured with Pearson coefficient.

**RESULTS**

We used the *ex vivo* organ culture model to explore the effects of Kv1.3 blockers against restenosis in human vessels. First, we tested the suitability of this model, characterizing the preservation of tissue viability and architecture after 2 weeks culture, and the effect of 20% FBS treatment to promote intimal hyperplasia. Both in hMA and in hSV, 20% FBS incubation for two weeks led to a marked inward remodeling of the vessel wall, characterized by an increased thickness of intimal and media layers and a concomitant decrease of the lumen area (Supplemental Figure IIA, B). Remodeling was consistently observed in 18 out of 21 hSV and in 18 out of 20 hMA, Both the intima to media ratio (I/M) and the percentage of stenosis[16] were significantly increased with FBS treatment (Supplemental Figure IIC). Information about the sex of the patients was available for the majority of donors, but due to the small number of female samples, data were analyzed for both sexes together. In the case of hSV, we did not find sex differences in remodeling (Supplemental Figure IIIA, B). However, the small number of cases and the differences also in age distribution between sexes (Supplemental Figure IIIC, D) precluded any further analysis.

Next, we determined the impact of treatment with Kv1.3 blockers on FBS-induced intimal hyperplasia. Incubation of hSV or hMA with the selective Kv1.3 blocker PAP-1 (100 nM) significantly reduced 20%FBS-induced intimal hyperplasic lesions (Figure 1A, B). PAP-1 treatment was without effect in vessels kept in 0% FBS. FBS-induced hMA remodeling was also prevented with 10 nM Margatoxin (MgTx, Figure 1C) another selective Kv1.3 blocker not structurally related to PAP-1, suggesting that these effects are due to Kv1.3 inhibition.

PM of VSMCs is the principal contributor to this vessel remodeling. Upon PM, VSMC dedifferentiate and show proliferative, migratory and secretory capabilities. We tried to identify the contribution of Kv1.3 blockade (using PAP-1) to these processes.

Cell proliferation was analyzed both in hMA rings kept in culture (by counting the number of Hoechst-labelled nuclei in the intima and media layer, figure 2A) or in primary VSMCs cultures from these arteries, using EdU staining (Figure 2B). In both cases, a significant decrease of the 20% FBS (or PDGF) induced proliferation was observed with 100 nM PAP-1. In VSMCs cultures, the same inhibition could be observed upon treatment with 10 nM MgTx, and with 20 µM PD98059, a potent MEK/ERK inhibitor. PD98059 effect was not additive with that of PAP-1, suggesting the involvement of MEK/ERK in the Kv1.3 signaling pathway, as described in other human VSMC cultures [13]. Migration of hMA VSMCs tested with two different methods (scratch assay and Boyden chamber) was also inhibited by 100 nM PAP-1 treatment (Figures 2C and 2D). Finally, as PM also associates with an increased secretion of ECM proteins, we explored whether Kv1.3 blockers could modulate ECM synthesis. Collagen (particularly types I and III) and elastin are the most abundant proteins in the ECM of the vessel walls[25]. Upon PM, an increase in collagen synthesis and deposition (collagen I in particular) together with an increased secretion and disorganization of elastin fibers have been reported [26,27]. Analysis and quantification of elastin autofluorescence shows an increased content upon 20% FBS incubation and a marked disorganization of the elastin structure (Figure 3A). Both effects are completely prevented in the presence of PAP-1. The same results were obtained with Orcein stain (not shown). To explore

changes in collagen expression, mRNA levels of the alpha subunit of collagen I and III (COL1A1 and COL3A1) were determined by qPCR. We also measured the mRNA expression levels of collagen VIII (COL8A1) a network-forming collagen type with increased expression in vascular remodeling in atherosclerosis models [28]. COL1A1 and COL3A1 expression increased with 20% FBS treatment and was reduced in the presence of PAP-1 (Figure 3B, left), while COL8A1 expression decreased in all experimental conditions. However, the changes in the amount of collagen mRNA were determined by the dominant expression of COL1A1 and COL3A1 (right graph, Figure 3B). Masson trichrome staining also showed an increased collagen content of arterial rings kept in 20% FBS, although in this case no significant effect of PAP-1 was seen (Figure 3C).

These results prompted us to explore the possible mechanisms involved in the regulation of PM through Kv1.3 activity. Extensive studies and developmental models suggest that myocardin (MYOCD) has a central role in regulating smooth muscle cells (SMC) phenotype and SMC-specific gene expression via SRF interaction. MYOCD expression associates with the contractile SMC phenotype, and its reduced expression/activity during PM is a key regulator of the neointima response [3,29,30]. MYOCD induces activation of SMC promoters and SMC marker genes, including some ion channels like Kcnmb1 [31]. Therefore, we explored whether Kv1.3 and/or Kv1.5 genes could be also MYOCD-regulated genes. First, we determined the expression levels of all Kv1 channels in human vessels, both in fresh tissue (contractile phenotype) and in VSMC culture (synthetic phenotype). As previously described in other preparations [9,23], our data confirmed the dominant expression of Kv1.5 in hMA tissue and the switch towards a prominent role of Kv1.3 in VSMC cultures (Figure 4A). MYOCD mRNA was highly expressed in hMA (t=0), and its levels significantly decreased after keeping the arterial rings in culture for two weeks. As expected, the decrease in MYOCD expression was larger when arterial rings or isolated VSMCs were cultured with 20% FBS (Figure 4B). We explored whether MYOCD changes were associated with changes in the expression of Kv1.3 and Kv1.5 channels in our experimental conditions. Calponin (Cnn) mRNA expression levels were also determined as a positive control for a MYOCD-regulated gene [32,33]. Figure 4D indicates a positive correlation between MYOCD mRNA expression and both Cnn and Kv1.5 mRNA levels. This correlation is absent when comparing MYOCD expression with Kv1.3, or with its accessory subunit Kv$\beta$2. Both showed little variation in all conditions tested. The apparent lack of regulation of Kv1.3 expression has been previously reported in human VSMCs cultures [13]. These data suggest that Kv1.5 mRNA expression may be regulated by MYOCD. In fact, changes in Kv1.5 expression follow the same pattern of MYOCD changes (Figure 4C). To extend these observations we also examined correlations between Kv1.5 (KCNA5) and MYOCD and SRF using RNA-Seq data downloaded from the GTExPortal.org. KCNA5 correlated significantly with MYOCD across human tissues (examples shown in Supplemental Figure IV, panels A-D). Correlations were strongest in gastrointestinal organs, but significant also in arteries, as exemplified by the coronary artery (panel D). SRF and KCNA5 similarly correlated at the mRNA level (panels E through H). Taken together, correlation analysis at the mRNA level in our organ cultured arteries, in VSMCs and using publicly accessible human expression data, support the hypothesis that Kv1.5 may be targeted by MYOCD/SRF (as depicted at the upper right, Fig. 4).

Kv1.5 channels have been shown to reduce proliferation in heterologous systems[12,15]. In native VSMC, we postulated that they may inhibit proliferation by occluding Kv1.3 channel signaling. To test this hypothesis, we designed viral vectors to overexpress fluorescently tagged Kv1.3 or Kv1.5 channels. The efficiency of infection was tested in hMA and hCA VSMCs in primary cultures. When infecting hMA VSMCs with AAV carrying GFP alone, Kv1.5-GFP or Kv1.3-Cherry, more than 90% of the cells showed reporter gene expression that could be detected in vivo (Figure 5A) or with GFP immunostaining (not shown). Electrophysiological studies in these cells demonstrated substantial expression of Kv1.5 or Kv1.3 currents (peak current density at +40 mV was 219.76 ±36 pA/pF for Kv1.3 and 149.27±25 pA/pF for Kv1.5 infected cells, versus 8.48 ±4 pA/pF in uninfected VSMCs or 2.58 ±2 pA/pF in GFP infected VSMCs, Figure 5A,B). Kv1.3 currents were identified by their sensitivity to PAP-1 (as shown in figure 5A, right panel) and also by their more negative activation threshold (-52.27 ± 1.8 mV) compared to Kv1.5 infected cells (-35.28 ±2.5 mV, figure 5B, bottom panel), as previously described [15,34]. Next, we studied VSMC proliferation in these cells. Kv1.3 infected cells have a higher proliferation rate than GFP-infected cells, whereas Kv1.5 overexpression significantly reduces proliferation rate, and abolished the inhibitory effect of PAP-1 treatment (Figure 5C). The increased proliferation rate of hMA VSMCs infected with Kv1.3 could not be reproduced by the Y447A mutant Kv1.3 channel (Kv1.3Y2, figure 5D), which has been described to abolish Kv1.3-induced proliferation in heterologous expression systems [15]. The effects of AAV-Kv1.5 infections were also reproduced with Lv-Kv1.5 infections. In Lv-Kv1.5-infected cells proliferation was not further inhibited by PAP-1 or by Kv1.5 blockers such as DPO, consistent with the hypothesis that Kv1.5 inhibits proliferation by occluding Kv1.3. Moreover, 20 µM PD98059 inhibited proliferation to the same level in Kv1.5 and GFP expressing cells (Supplemental Figure V). We also explored the effect of AAV infections on hMA VSMCs migration using a scratch assay (Figure 5E). Whilst Kv1.5 overexpression inhibited cell migration, Kv1.3 or a poreless mutant (Kv1.3WF) highly increased it.

AAV-Kv1.5 and AAV-GFP vectors were also used for infection of hMA rings in organ culture. The efficiency of infection was confirmed by direct visualization of GFP in confocal images of arterial sections, by determining GFP mRNA expression levels in the samples or by immunolabelling with GFP (Supplemental Figure VI) and Kv1.5 antibodies (Figure 6A). After 14 days in culture, we found that AAV-Kv1.5 infections prevented 20%FBS-induced remodeling to the same extent as PAP-1 treatment. Again, these two effects were not additive, suggesting a common pathway (Figure 6B). Similar results were obtained when proliferation was measured in the arterial rings by counting cell nuclei (Supplemental Figure VII). Additionally, infection of hMA rings with a Lv-ccMYOCD induced knock-down of myocardin (Figure 6C), together with a pronounced vessel remodeling in 0% FBS (Figure 6D). Due to the concerns regarding specificity of myocardin antibodies [35], we also explored expression of other myocardin target genes (MYHII and SM22), which were also decreased. (Supplemental Figure VIII). Finally, control experiments to exclude possible off-target effects of Lv-ccMYOCD were also performed (supplemental Figure IX). In both groups of infected vessels, we determined the mRNA expression levels of myocardin, Cnn and Kv1.5 mRNA (Figure 6E). MYOCD expression decreased when arterial rings were cultured in the presence of 20% FBS and was unchanged by Kv1.5 overexpression in AAV-Kv1.5 infected samples. However, MYOCD knock-down in Lv-ccMYOCD infected rings

decreased both calponin and Kv1.5 mRNA expression (and also Kv1.5 protein expression, see Figure 6C). We conclude that MYOCD expression does not depend of Kv1.5, but Kv1.5 behaves like a MYOCD regulated gene. Consistent with these observations, overexpression of myocardin in hCASMCs using adenoviral vectors led to a significant upregulation of Kv1.5 mRNA, which was only partially reproduced by MRTF-B infection (Figure 6E). The expression levels of αSMA, a known myocardin target, were also determined in the same samples as a positive control (Figure 6F).

## DISCUSSION

In this study we identified Kv1.3 channel activity as a modulator of human VSMC dedifferentiation, migration and proliferation. Our results uncovered several major findings. First, using human vessels (mammary arteries and saphenous veins) in organ culture, we demonstrated that inhibition of Kv1.3 channels can prevent unwanted remodeling. Second, we provided evidence suggesting that MYOCD-dependent expression of Kv1.5 channels, via modulation of the Kv1.3/Kv1.5 ratio in VSMCs, underlies the changes in the functional contribution of Kv1.3 channels to PM. Third, by using viral vectors to overexpress Kv1.5 and Kv1.3 (WT or mutant) channels we demonstrated that Kv1.5 channels inhibit vascular remodeling by occluding Kv1.3 activity. We propose that upon PM reduction of Kv1.5 uncovers Kv1.3-dependent signaling pathways leading to proliferation and migration. Altogether, these data indicated that blockade of Kv1.3, either with selective inhibitors or with Kv1.5 overexpression could represent an effective novel strategy for the prevention of intimal hyperplasia in human vessels in vivo.

Kv1.3 channel have been shown to be involved in cell proliferation in many cell types, including immune system cells, glial cells, VSMCs and cancer cells [36]. With the exception of T-lymphocytes, all these cells express other Kv1 channels, whose levels are also altered upon activation. Specifically, downregulation of Kv1.5 channels often associates with Kv1.3 upregulation in proliferating cells [13,37,38]. On these grounds, we proposed that the relative amount of these two channels (the Kv1.3/Kv1.5 ratio) could represent the master switch determining the Kv1 channel effect on proliferation. In several human and mouse vessels we have previously found a dramatic decrease of Kv1.5 expression upon PM or in response to mitogens, with no significant changes in Kv1.3 expression [12,13]. Here, we confirmed this notion in organ culture experiments of human vessels. There is a clear relationship between Kv1.5 mRNA levels and PM; in fact, we show for the first time that Kv1.5 expression is regulated by myocardin. Myocardin knock-down decreased expression of Kv1.5 and myocardin overexpression increases it, while Kv1.5 overexpression inhibits PM without affecting myocardin expression (Figure 6). Altogether, these data indicated that not only there is a correlation between myocardin and Kv1.5 expression levels but also that Kv1.5 expression is regulated by myocardin, confirming our hypothesis that Kv1.5 is another SM-specific differentiation marker, in the same way as other contractile proteins. Indeed, when we leveraged publicly accessible human RNA-Seq data (GTExPortal.org) for correlation analysis, highly significant correlations were found in several tissues including the coronary artery. In addition, Kv1.5 expression shows a very high expression in heart and arteries (https://gtexportal.org/home/gene/KCNA5), and seems to be mainly located in cardiac and smooth muscle.

These data suggest that Kv1.5 downregulation is the relevant change for PM and VSMC proliferation. We propose that two mechanisms can underlie Kv1.5-mediated inhibition of PM: activation of antiproliferative signaling pathways and/or prevention of Kv1.3-induced proliferation. Heterologous expression of Kv1.5 in HEK cells inhibits proliferation, supporting the first option [12,15]. However, this may not be the case in native systems, where Kv1.3 and Kv1.5 are likely to form heteromultimeric channels, as has been described for several Kv1 channels [39–41]. Here we demonstrate that Kv1.5

overexpression inhibits PM both in organ culture and in cultured VSMCs (Figures 5-6). In both preparations, the effects of Kv1.5 overexpression can be reproduced with Kv1.3 blockade, and the two effects are non-additive. The interference of Kv1.5 with the pro-proliferative signaling pathways activated by Kv1.3 protein is the simplest explanation for these data.

In addition, adenoviral expression of mutant Kv1.3 channels provided some other relevant conclusions regarding the mechanisms involved in Kv1.3 induced proliferation of VSMCs. Initially, we could think of two non-exclusive mechanisms: either VSMCs use Kv1.3 channels to regulate resting membrane potential (and hence cell cycle), or Kv1.3 channels may serve as sensors of changes in membrane potential, acting as a signaling molecule connecting bioelectrical signals with intracellular pathways. In heterologous systems, $K^+$ fluxes through Kv1.3 channel are not required for proliferation, but the response needs a voltage-dependent conformational change of the channel [12]. The effect of overexpressing the Kv1.3 poreless channel (Kv1.3WF, Figure 5E) indicates that, also in VSMCs, $K^+$ fluxes are not required for Kv1.3-induced proliferation. Moreover, it has been reported that at least two single phosphorylation sites in the C-terminal region of the channel could recapitulate Kv1.3-induced proliferation, as their individual mutation abolished the effect [15]. Here, we found that overexpression of Kv1.3 (but not of the phosphorylation-deficient channel Kv1.3Y2), increased VSMCs proliferation, indicating the requirement for interaction of Kv1.3 protein with other partners (via phosphorylation of the channel) to activate proliferation. Altogether, our data suggest that there is a specific requirement for Kv1.3 channel protein to facilitate proliferation, regardless of Kv1.3 channel ion flux. The nature of these interacting proteins and the detailed molecular mechanisms activating Kv1.3-induced proliferation await future research.

In addition to providing relevant information regarding the mechanisms contributing to PM, our work has another relevant added value: exploring these mechanisms in the remodeling of human vessels. The reduction of in-stent restenosis of both rapamycin- and paclitaxel-eluting stents has translated into their widespread use. However, their lack of specificity with the subsequent failure of healing [42] calls for the development of newer agents and/or polymers for stent coverings. In this scenario, we propose a novel strategy (Kv1.3 channel blockade) whose efficacy has been previously tested in animal lesion models. However, it is well known that these models have many limitations: they are not restenosis models, neointima formation is not always associated with lumen narrowing, rodent vessels do not behave like human vessels and healthy vessels do not behave like diseased vessels, because of differences in cell cycle regulation between dedifferentiated VSMCs in the lesion and normal VSMCs [43,44]. Using the same human vessels that are commonly used for coronary angioplasty, we demonstrate here that local Kv1.3 channel blockade (by application of selective inhibitors or by Kv1.5 overexpression) is an efficient strategy to prevent vascular remodeling. These interventions inhibit neointima formation by reducing VSMC proliferation and migration and ECM production. It is likely that they could also reduce remodeling by acting on other targets aside from VSMCs. Kv1.3 blockers modulate the immune responses [45], have anti-inflammatory effects by inhibiting migration, proliferation and NOS expression in macrophages [46], and can exert anti-thrombotic effects [47]. Thus, by targeting several biological processes involved in restenosis (inhibiting PM of VSMCs,

decreasing fibrosis, inflammation and platelet aggregation), Kv1.3 inhibitors could represent very good candidates for the prevention of unwanted remodeling in human vessels.

**ACKNOWLEDGMENTS**

We thank Esperanza Alonso for excellent technical assistance. We are in debt with Drs A. San Román, J López Díaz and all the personnel of the Cardiac Surgery Unit of the Hospital Clínico Universitario de Valladolid for their wiliness to provide all the arterial samples for this study. We are also grateful to COLMAH collection for the use of human primary VSMCs cultures, and to all the members of the lab for their helpful discussions.

**SOURCES OF FUNDING**

This work was supported by grant BFU2016-75360-R from the Ministerio de Economía y Competitividad (MINECO), to MTPG and JRLL and Junta de Castilla y León Grant VA114P17 to MTPG. MAM and JS are predoctoral fellows of the UVa-Santander. KS was supported by the Swedish Research Council (2017-01225_3).

**DISCLOSURES**

None

**REFERENCES**


1. Alexander MR, Owens GK. Epigenetic Control of Smooth Muscle Cell Differentiation and Phenotypic Switching in Vascular Development and Disease. *Annu Rev Physiol*. 2012;74:13-40.
2. Bennett MR, O'Sullivan M. Mechanisms of angioplasty and stent restenosis: implications for design of rational therapy. *Pharmacol Ther*. 2001;91:149-166.
3. Miano JM, Long X, Fujiwara K. Serum response factor: master regulator of the actin cytoskeleton and contractile apparatus. *Am J Physiol Cell Physiol*. 2007;292:C70-C81.
4. Long X, Bell RD, Gerthoffer WT, Zlokovic B V., Miano JM. Myocardin is sufficient for a smooth muscle-like contractile phenotype. *Arterioscler Thromb Vasc Biol*. 2008;28:1505-1510.
5. Kawai-Kowase K, Owens GK. Multiple repressor pathways contribute to phenotypic switching of vascular smooth muscle cells. *Am J Physiol Cell Physiol*. 2007;292:C59-C69.
6. Dens JA, Desmet WJ, Coussement P, De Scheerder IK, Kostopoulos K, Kerdsinchai P, Supanantaroek C, Piessens JH. Usefulness of nisoldipine for prevention of restenosis after percutaneous transluminal coronary angioplasty. *Am J Cardiol*. 2001;87:28-33.
7. Acute platelet inhibition with abciximab does not reduce in-stent restenosis. The ERASER Investigators. *Circulation*. 1999;100:799-806.
8. Schühlen H, Kastrati A, Mehilli J, Hausleiter J, Dirschinger J, Dotzer F, Bollwein H, Schömig A. Abciximab and angiographic restenosis after coronary stent placement. Analysis of the angiographic substudy of ISAR-REACT-A double-blind, placebo-controlled, randomized trial evaluating abciximab in patients undergoing elective percutaneous coronary interventions after pretreatment with a high loading dose of clopidogrel. *Am Heart J*. 2006;151:1248-1254.
9. Cidad P, Moreno-Domínguez A, Novensá L, Roqué M, Barquín L, Heras M, Pérez-García MTT, López-López JR. Characterization of ion channels involved in the proliferative response of femoral artery smooth muscle cells. *Arterioscler Thromb Vasc Biol*. 2010;30:1203-1211.
10. Cheong A, Li J, Sukumar P, Kumar B, Zeng F, Riches K, Munsch C, Wood IC, Porter KE, Beech DJ. Potent suppression of vascular smooth muscle cell migration and human neointimal hyperplasia by KV1.3 channel blockers. *Cardiovasc Res*. 2011;89:282-289.
11. Cidad P, Novensà L, Garabito M, Batlle M, Dantas APP, Heras M, López-López JR, Pérez-García MT, Roqué M, Pérez-García MT, Roqué M, Pérez-García MT, Roqué M. K+ Channels Expression in Hypertension After Arterial Injury, and Effect of Selective Kv1.3 Blockade with PAP-1 on Intimal Hyperplasia Formation. *Cardiovasc Drugs Ther*. 2014;28:501-511.
12. Cidad P, Jiménez-Pérez L, García-Arribas D, Miguel-Velado E, Tajada S, Ruiz-Mcdavitt C, López-López JR, Pérez-García MT. Kv1.3 channels can modulate cell proliferation during phenotypic switch by an ion-flux independent mechanism. *Arterioscler Thromb Vasc Biol*. 2012;32:1299-1307.
13. Cidad P, Miguel-Velado E, Ruiz-McDavitt C, Alonso E, Jiménez-Pérez L, Asuaje A, Carmona Y, García-Arribas D, López J, Marroquín Y, Fernández M, Roqué M, Pérez-García MT, López-López JR. Kv1.3 channels modulate human vascular

smooth muscle cells proliferation independently of mTOR signaling pathway. *Pflügers Arch - Eur J Physiol*. 2015;467:1711-1722.
14. Thorneloe KS, Chen TT, Kerr PM, Grier EF, Horowitz B, Cole WC, Walsh MP. Molecular composition of 4-aminopyridine-sensitive voltage-gated K(+) channels of vascular smooth muscle. *Circ Res*. 2001;89:1030-1037.
15. Jiménez-Pérez L, Cidad P, Álvarez-Miguel I, Santos-Hipólito A, Torres-Merino R, Alonso E, de la Fuente MÁ, López-López JR, Pérez-García MT. Molecular Determinants of Kv1.3 Potassium Channels-Induced Proliferation. *J Biol Chem* . 2015;291:1-13.
16. Roque M, Fallon JT, Badimon JJ, Zhang WX, Taubman MB, Reis ED. Mouse model of femoral artery denudation injury associated with the rapid accumulation of adhesion molecules on the luminal surface and recruitment of neutrophils. *Arterioscler Thromb Vasc Biol*. 2000;20:335-342.
17. Ma Z. Total RNA Extraction from Formalin-Fixed, Paraffin-Embedded (FFPE) Blocks. *BIO-PROTOCOL*. 2012;2:e161.
18. Aurnhammer C, Haase M, Muether N, Hausl M, Rauschhuber C, Huber I, Nitschko H, Busch U, Sing A, Ehrhardt A, Baiker A. Universal Real-Time PCR for the Detection and Quantification of Adeno-Associated Virus Serotype 2-Derived ITR sequences. *Hum Gene Ther Methods*. 2012;23:18-28.
19. Boehm E, Zornoza M, Jourdain AA, Delmiro Magdalena A, García-Consuegra I, Torres Merino R, Orduña A, Martín MA, Martinou J-C, De la Fuente MA, Simarro M. Role of FAST Kinase Domains 3 (FASTKD3) in Post-transcriptional Regulation of Mitochondrial Gene Expression. *J Biol Chem*. 2016;291:25877-25887.
20. Krawczyk KK, Yao Mattisson I, Ekman M, Oskolkov N, Grantinge R, Kotowska D, Olde B, Hansson O, Albinsson S, Miano JM, Rippe C, Swärd K. Myocardin Family Members Drive Formation of Caveolae. Nabi IR, ed. *PLoS One*. 2015;10:e0133931.
21. Zhu B, Rippe C, Holmberg J, Zeng S, Perisic L, Albinsson S, Hedin U, Uvelius B, Swärd K. Nexilin/NEXN controls actin polymerization in smooth muscle and is regulated by myocardin family coactivators and YAP. *Sci Rep*. 2018;8:13025.
22. Haeussler M, Schönig K, Eckert H, Eschstruth A, Mianné J, Renaud J-B, Schneider-Maunoury S, Shkumatava A, Teboul L, Kent J, Joly J-S, Concordet J-P. Evaluation of off-target and on-target scoring algorithms and integration into the guide RNA selection tool CRISPOR. *Genome Biol*. 2016;17:148.
23. Miguel-Velado E, Moreno-Domínguez A, Colinas O, Cidad P, Heras M, Pérez-García MT, López-López JR. Contribution of Kv channels to phenotypic remodeling of human uterine artery smooth muscle cells. *Circ Res*. 2005;97:1280-1287.
24. Liu S, Yang Y, Jiang S, Xu H, Tang N, Lobo A, Zhang R, Liu S, Yu T, Xin H. MiR-378a-5p Regulates Proliferation and Migration in Vascular Smooth Muscle Cell by Targeting CDK1. *Front Genet*. 2019;10:22.
25. Wagenseil JE, Mecham RP. Vascular Extracellular Matrix and Arterial Mechanics. *Physiol Rev*. 2009;89:957-989.
26. Karnik SK, Brooke BS, Bayes-Genis A, Sorensen L, Wythe JD, Schwartz RS, Keating MT, Li DY. A critical role for elastin signaling in vascular morphogenesis and disease. *Development*. 2003;130:411-423.
27. Wong CY, Rothuizen TC, de Vries MR, Rabelink TJ, Hamming JF, van Zonneveld

AJ, Quax PHA, Rotmans JI. Elastin is a Key Regulator of Outward Remodeling in Arteriovenous Fistulas. *Eur J Vasc Endovasc Surg*. 2015;49:480-486.
28. Lopes J, Adiguzel E, Gu S, Liu S-L, Hou G, Heximer S, Assoian RK, Bendeck MP. Type VIII Collagen Mediates Vessel Wall Remodeling after Arterial Injury and Fibrous Cap Formation in Atherosclerosis. *Am J Pathol*. 2013;182:2241-2253.
29. Owens GK. Molecular control of vascular smooth muscle cell differentiation and phenotypic plasticity. *Novartis Found Symp*. 2007;283:174-91.
30. Talasila A, Yu H, Ackers-Johnson M, Bot M, van Berkel T, Bennett MR, Bot I, Sinha S. Myocardin Regulates Vascular Response to Injury Through miR-24/-29a and Platelet-Derived Growth Factor Receptor-β. *Arterioscler Thromb Vasc Biol*. 2013;33:2355-2365.
31. Long X, Tharp DL, Georger MA, Slivano OJ, Lee MY, Wamhoff BR, Bowles DK, Miano JM. The smooth muscle cell-restricted KCNMB1 ion channel subunit is a direct transcriptional target of serum response factor and myocardin. *J Biol Chem*. 2009;284:33671-33682.
32. Chen J, Kitchen CM, Streb JW, Miano JM. Myocardin: A Component of a Molecular Switch for Smooth Muscle Differentiation. *J Mol Cell Cardiol*. 2002;34:1345-1356.
33. Du KL, Ip HS, Li J, Chen M, Dandre F, Yu W, Lu MM, Owens GK, Parmacek MS. Myocardin is a critical serum response factor cofactor in the transcriptional program regulating smooth muscle cell differentiation. *Mol Cell Biol*. 2003;23:2425-2437.
34. Coetzee W a, Amarillo Y, Chiu J, Chow a, Lau D, McCormack T, Moreno H, Nadal MS, Ozaita a, Pountney D, Saganich M, Vega-Saenz de Miera E, Rudy B. Molecular diversity of K+ channels. *Ann N Y Acad Sci*. 1999;868:233-285.
35. Lyu Q, Dhagia V, Han Y, Guo B, Wines-Samuelson ME, Christie CK, Yin Q, Slivano OJ, Herring P, Long X, Gupte SA, Miano JM. CRISPR-Cas9-Mediated Epitope Tagging Provides Accurate and Versatile Assessment of Myocardin-Brief Report. *Arterioscler Thromb Vasc Biol*. 2018;38:2184-2190.
36. Pérez-García MT, Cidad P, López-López JR. The secret life of ion channels: Kv1.3 potassium channels and proliferation. *Am J Physiol - Cell Physiol*. 2018;314:C27-C42.
37. Kotecha SA, Schlichter LC. A Kv1.5 to Kv1.3 switch in endogenous hippocampal microglia and a role in proliferation. *J Neurosci*. 1999;19:10680-10693.
38. Vautier FF, Belachew S, Chittajallu R, Gallo V. Shaker-type potassium channel subunits differentially control oligodendrocyte progenitor proliferation. *Glia*. 2004;48:337-345.
39. Sobko A, Peretz A, Shirihai O, Etkin S, Cherepanova V, Dagan D, Attali B. Heteromultimeric Delayed-Rectifier K+ Channels in Schwann Cells: Developmental Expression and Role in Cell Proliferation. *J Neurosci*. 1998;18:10398-408.
40. Plane F, Johnson R, Kerr P, Wiehler W, Thorneloe K, Ishii K, Chen T, Cole W. Heteromultimeric Kv1 channels contribute to myogenic control of arterial diameter. *Circ Res*. 2005;96:216-224.
41. Pannasch U, Farber K, Nolte C, Blonski M, Yan Chiu S, Messing A, Kettenmann H, Färber K, Nolte C, Blonski M, Yan Chiu S, Messing A, Kettenmann H. The potassium channels Kv1.5 and Kv1.3 modulate distinct functions of microglia.

*Mol Cell Neurosci*. 2006;33:401-411.
42. Lüscher TF, Steffel J, Eberli FR, Joner M, Nakazawa G, Tanner FC, Virmani R. Drug-Eluting Stent and Coronary Thrombosis. *Circulation*. 2007;115:1051-1058.
43. O'Sullivan M, Scott SD, McCarthy N, Figg N, Shapiro LM, Kirkpatrick P, Bennett MR. Differential cyclin E expression in human in-stent stenosis smooth muscle cells identifies targets for selective anti-restenosis therapy. *Cardiovasc Res*. 2003;60:673-683.
44. Calvert PA, Bennett MR. Restenosis Revisited. *Circ Res*. 2009;104:823-825.
45. Feske S, Wulff H, Skolnik EY. Ion channels in innate and adaptive immunity. *Annu Rev Immunol*. 2015;33:291-353.
46. Vicente R, Escalada A, Coma M, Fuster G, Sánchez-Tilló E, López-Iglesias C, Soler C, Solsona C, Celada A, Felipe A. Differential voltage-dependent K+ channel responses during proliferation and activation in macrophages. *J Biol Chem*. 2003;278:46307-46320.
47. McCloskey C, Jones S, Amisten S, Snowden RT, Kaczmarek LK, Erlinge D, Goodall AH, Forsythe ID, Mahaut-Smith MP. Kv1.3 is the exclusive voltage-gated K+ channel of platelets and megakaryocytes: roles in membrane potential, Ca2+ signalling and platelet count. *J Physiol*. 2010;588:1399-1406.

**HIGHLIGHTS**

1. Kv1.3 channel blockade prevented remodeling of human vessels in organ culture by inhibiting VSMC proliferation and migration and ECM secretion.
2. Kv1.3 channel behaves as a housekeeping gene, while Kv1.5 channel is a myocardin-regulated, VSMC contractile marker. The increased functional contribution of Kv1.3 channels in dedifferentiated VSMCs is a consequence of the myocardin-dependent downregulation of Kv1.5 channels.
3. Kv1.5 overexpression inhibited human vessels remodeling by hampering Kv1.3-induced migration and proliferation.
4. Inhibition of Kv1.3 channel function with selective blockers or by preventing Kv1.5 downregulation can represent an effective strategy for the prevention of intimal hyperplasia in human vessels.

## FIGURE LEGENDS

### Figure 1. Kv1.3 blockers inhibited FBS-induced vascular remodeling.

**A**. Representative microphotographs of hSV kept in organ culture for two weeks in serum free conditions (0FBS), or in the presence of 20% Fetal bovine serum (20FBS) alone or combined with PAP-1 (100 nM). Images were taken with a 10X objective (NA=0.3). L = lumen side. The black arrows indicated the thickness of the intima layer, and the arrowheads the media/adventitia border. The average data (mean ±SEM) of the intima/media ratio obtained in 12 different vessels is represented in the right plot. **B**. A similar experiment carried out in hMA in the same experimental conditions. hMA do not present intima layer in the absence of FBS. The bars plot shows average data of 8-15 arteries. Notice the lack of remodeling and the absence of effect of PAP-1 treatment in 0FBS conditions, compared to control vessels not maintained in organ culture (t=0). **C.** Representative microphotographs of the inhibitory effect of MgTx (10nM) on 20% FBS-induced remodeling of hMA. Summary data were obtained from 4 arteries. * p<0.05; **p<0.01; ***p<0.001 with respect to 20%FBS, for paired data. Scale bar=100 µm.

### Figure 2. Kv1.3 blockers inhibited proliferation and migration.

**A.** Number of nuclei present in the intima and media layer of hMA rings kept in control conditions (0% FBS), with 20% FBS alone or in the presence of 100 nM PAP-1. hMA sections were stained with Hoechst, and the nuclei present in the intima and media layer in four, 225 µm wide sections for each sample were counted. Representative images (10X objective) are depicted as an inset (Scale bar = 100 µm). L = lumen side. Bars plot shows the mean ± SEM of 4-10 arteries in the indicated conditions. ** p<0.01; ***p<0.001 with respect to 20% FBS. **B.** Proliferation of hMA VSMC in primary culture was determined by EdU incorporation, after a 24h treatment in serum free conditions (0FBS) or in the presence of 20ng/ml PDGF alone or in combination with the indicated drugs (PAP-1 100nM; Margatoxin 10 nM; PD98059 20µM). Each data bar is the mean ± SEM of 12-40 individual determinations obtained in at least 5 independent experiments. Positive and negative controls were included in all experiments. ***p<0.001 with respect to PDGF alone. **C.** Representative examples of a scratch migration assay in control conditions (left) or in the presence of PAP-1 (right) and bars plot with the summary data of the percentage of invaded area at 4h. Each bar is the average ± SEM of 18 individual experiments from 7 different primary VSMCs cultures. ***p<0.001. **D.** Data of Boyden chamber migration assay representing the cell number that migrated to the lower side of the chamber after 18h of treatment. Mean ±SEM, n=9. ***p<0.001 with respect to 20%FBS.

### Figure 3. Kv1.3 blockade inhibited ECM secretion in organ culture.

**A.** Microphotographs of rings of the same hMA incubated in the indicated conditions, showing elastic lamina auto-fluorescence in green and Hoechst stained nuclei in blue. Images were taken with a 20X objective (NA=0.5). Scale bar = 100µm. The elastin area labelled was quantified (see methods) and average data of 9 experiments (Mean ± SEM) is shown in the plot. *p<0.05, **p<0.01 compared with 20% FBS, paired data. **B.** mRNA expression of COL1A1, COL3A1 and COL8A1 genes was determined in hMA rings in control conditions (t=0) or after 2 weeks in organ culture in the indicated conditions. RPL18 was used as housekeeping gene to obtain mRNA amount ($2^{-\Delta Ct}$, right). Also, data were normalized to the t=0 condition with the $2^{-\Delta\Delta Ct}$ relative quantification method, where $\Delta\Delta Ct = \Delta Ct_{experimental} - \Delta Ct_{calibrator}$ (left). Data are mean± SEM obtained from triplicates of at least 5 different samples. *p<0.05 compared to 20% FBS. **C.** An estimation of the collagen content was obtained by quantifying the green-stained area of intima and media layers using the Masson trichrome. Representative microphotographs (scale bar = 100 µm, 10X objective) and pooled data (Mean ± SEM, n=9). *p<0.05 compared to 20%FBS. L = lumen side.

**Figure 4. Kv1.5 (but not Kv1.3) mRNA expression correlates with Myocardin.**
**A.** Relative mRNA abundance of the voltage-dependent potassium channel Kv1 family genes in contractile (tissue) and proliferating (culture) VSMC from human mammary arteries. Expression levels were normalized with respect to RPL18 and expressed as $2^{-\Delta Ct}$, where $\Delta Ct=C_{tchannel}-Ct_{L18s}$. Each bar is the mean of 4 to 6 determinations from different donors obtained in triplicate assays. The relative abundance (in %) of each Kv1 subfamily member in both conditions is indicated in the bars plot and also illustrated in the pie-charts. **B, C.** Real time qPCR with Taqman probes were used to determine mRNA expression of Myocardin (**B**) and KCNA5 (the Kv1.5 gene, **C**). In both cases, mRNA abundance is expressed as $2^{-\Delta Ct}$, relative to RPL18. mRNA was obtained from fresh untreated arterial rings (t=0), arterial rings kept 2 weeks in organ culture in the indicated conditions and from cultured hMA VSMCs. In both graphs, * p<0.05, **p<0.01, ***p<0.001 with respect to untreated tissue (t=0) and $= p<0.05 compared with 0% FBS samples (n=8-10 determinations). **D.** The graphs show the correlation in each sample (n=30 for each data set) between the relative abundance of MYOCD and the relative abundance of KCNA5 (Kv1.5, black triangles) and CNN1 (Calponin, grey circles, upper plot) or KCNA3 (Kv1.3, open circles) and KCNAB2 (Kvβ2, black squares, lower graph). The lines show the fit of the data to a linear function. Pearson correlation coefficients were 0.83 (Calponin), 0.765 (Kv1.5), 0.15 (Kv1.3) and -0.19 (KCNAB2).

**Figure 5. Characterization of AAV-mediated overexpression of Kv1.3 and Kv1.5 in hMA VSMCs.**
**A.** Representative current-voltage (I/V) curves obtained in hMA VSMCs infected with AAV-GFP, AAV-Kv1.5 (Kv1.5-GFP) and AAV-Kv1.3 (Kv1.3-Cherry). Currents were elicited by pulses from -60 to +60 mV in 10 mV steps. The current traces elicited are shown in each case. For Kv1.3, the I/V curve obtained in the presence of 100 nM PAP is also shown. The microphotographs show efficiency of the infections by direct visualization of the fluorescent tags. **B.** (top) Bar plot showing peak current density (pA/pF) at +40mV obtained in control cells and in cells infected with the three types of AAV. N= 8-11 cells in each group from at least 3 independent experiments. The bar plot at the bottom shows the activation threshold estimated in the same conditions. Only Kv1.3-overexpressing VSMCs showed a shift towards a more negative threshold. Data are Mean ± SEM of 6-9 cells in each group. **C.** Effect of AAV-mediated overexpression on cell proliferation. Proliferation rate was calculated as the percentage of cells incorporating EdU. hMA VSMCs infected with AAV-GFP, AAV-Kv1.3 or AAV-Kv1.5 were incubated for 30 h with PDGF (20 ng/ml) alone or in combination with 100 nM PAP-1. EdU reagent was added to the media during the last 6 h of incubation. Each bar is mean ± SEM of 12-25 individual determinations from at least 4 independent experiments. **p<0.01, ***p<0.001 compared to control (GFP); $ p<0.05, $$$p<0.001 compared to their own control (PAP-untreated VSMCs). **D.** Proliferation rate obtained in another set of experiments exploring the effect of overexpression of Kv1.3 phosphorylation-defective mutant (Y2). N = 12-22 independent experiments from 5-10 different cultures. **E.** Scratch assay was used to determine the time course of migration of AAV-infected hMA VSMCs overexpressing GFP, Kv1.5, Kv1.3 or a poreless Kv1.3 mutant (WF). Mean ± SEM, n=4. *p<0.05, **p<0.01 compared to control, GFP-infected VSMCs; $ p<0.05 compared to Kv1.3.

**Figure 6. Overexpression of Kv1.5 channel reduces intimal hyperplasia in hMA.**
**A**. Immunohistochemical labelling ofKv1.5 in paraffin-embedded cross-sections from hMA infected with AAV-GFP or AAV-Kv1.5 and kept in organ culture with 20% FBS. 20X objective, scale bar = 100μm. **B.** Effect of Kv1.5 overexpression on intimal hyperplasia induced by 20% FBS. Intima to media ratio was calculated in control samples (GFP-0%FBS) or in GFP or Kv1.5-infected samples incubated with 20% FBS alone or in combination with PAP-1 (100nM) as indicated. Each bar is the mean ± SEM of 3-6 experiments. *p<0.05, **p<0.01, ***p<0.001 compared to 0% FBS-GFP. Representative microphotographs of hMA sections stained with

Masson trichrome in the three indicated conditions are shown in the left. Scale bar = 100μm. **C.** Immunohistochemical labelling for Myocardin (upper panels) and Kv1.5 (lower panels) of paraffin-embedded cross-sections of hMA infected with Lv-GFP (left and right panels) or the myocardin knock-down Lv-ccMYOCD (middle panels). Arterial rings were kept in organ culture for 14 days in 0% FBS or 20% FBS (right upper panel). Right bottom panel show the negative control for the Kv1.5 labelling in a GFP-0% FBS sample. 10X objective, scale bar 100μm. **D.** Effect of Myocardin knock-down on PM. Bar plot represents average data (mean ±SEM) of the intima/media ratio obtained in Lv-GFP-infected vessels kept in 0% FBS or 20% FBS or Lv-ccMYOCD-infected vessels kept in 0%FBS (middle bar); n=3. Representative microphotographs of the GFP and ccMYOCD-infected vessels in are depicted in the right. Arrows indicate neointima, scale bar 100μm. **E.** The left panel shows qPCR determination of the relative amount of Myocardin or endogenous Kv1.5 mRNA in hMA infected with AAV-GFP (kept in 0% or 20%FBS) or AAV-Kv1.5 (in 20%FBS) as in B. The right plot shows mRNA expression of myocardin, Kv1.5 or calponin in hMA infected with Lv-GFP (in 0% and 20%FBS) or Lv-ccMYOCD (in 0%FBS) as in D. Data are Mean ± SEM of 3- 5 independent experiments. ** p<0.01; ***p<0.001 with respect to 0%FBS-GFP. **F, G.** mRNA expression of Kv1.5 (**F**) and smooth muscle actin (αSMA, **G**), were determined in hCASMCs transduced with a null adenovirus vector (control) or with adenovirus overexpressing MYOCD, MRTF-A and MRTF-B as indicated. 18s was used as housekeeping gene to obtain mRNA amount and data were normalized to the control condition with the $2^{-\Delta\Delta Ct}$ relative quantification method, where $\Delta\Delta Ct = \Delta Ct_{experimental} - \Delta Ct_{control}$. Data are mean± SEM obtained from duplicates of 5 different infections. *p<0.05; ** p<0.01; ***p<0.001 with respect to control.

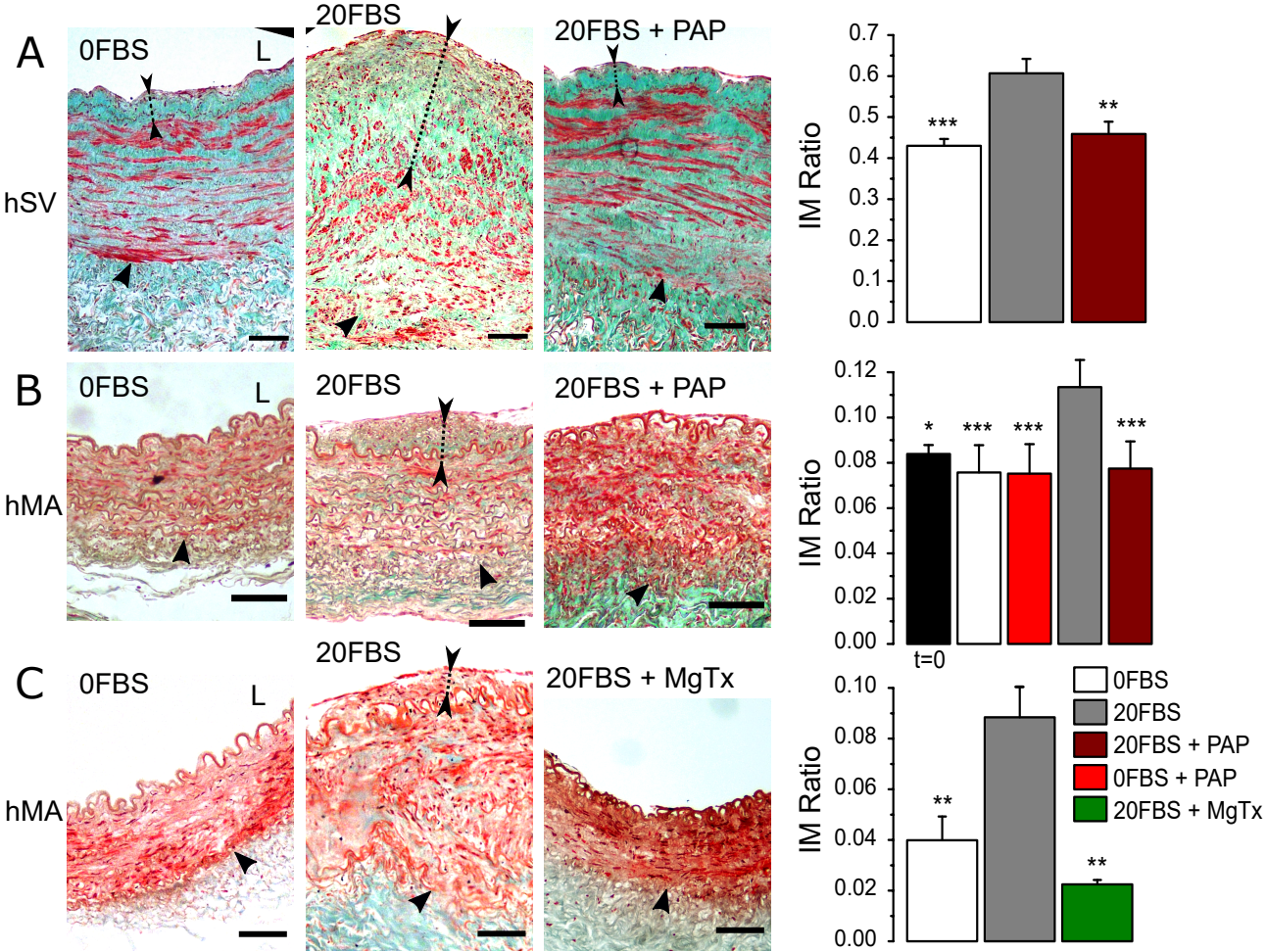
A
0FBS
L
20FBS
20FBS + PAP
hSV
IM Ratio
0.7
0.6
0.5
0.4
0.3
0.2
0.1
0.0
***
**
B
0FBS
L
20FBS
20FBS + PAP
hMA
IM Ratio
0.12
0.10
0.08
0.06
0.04
0.02
0.00
*
***
***
***
t=0
C
0FBS
L
20FBS
20FBS + MgTx
hMA
IM Ratio
0.10
0.08
0.06
0.04
0.02
0.00
**
**
0FBS
20FBS
20FBS + PAP
0FBS + PAP
20FBS + MgTx

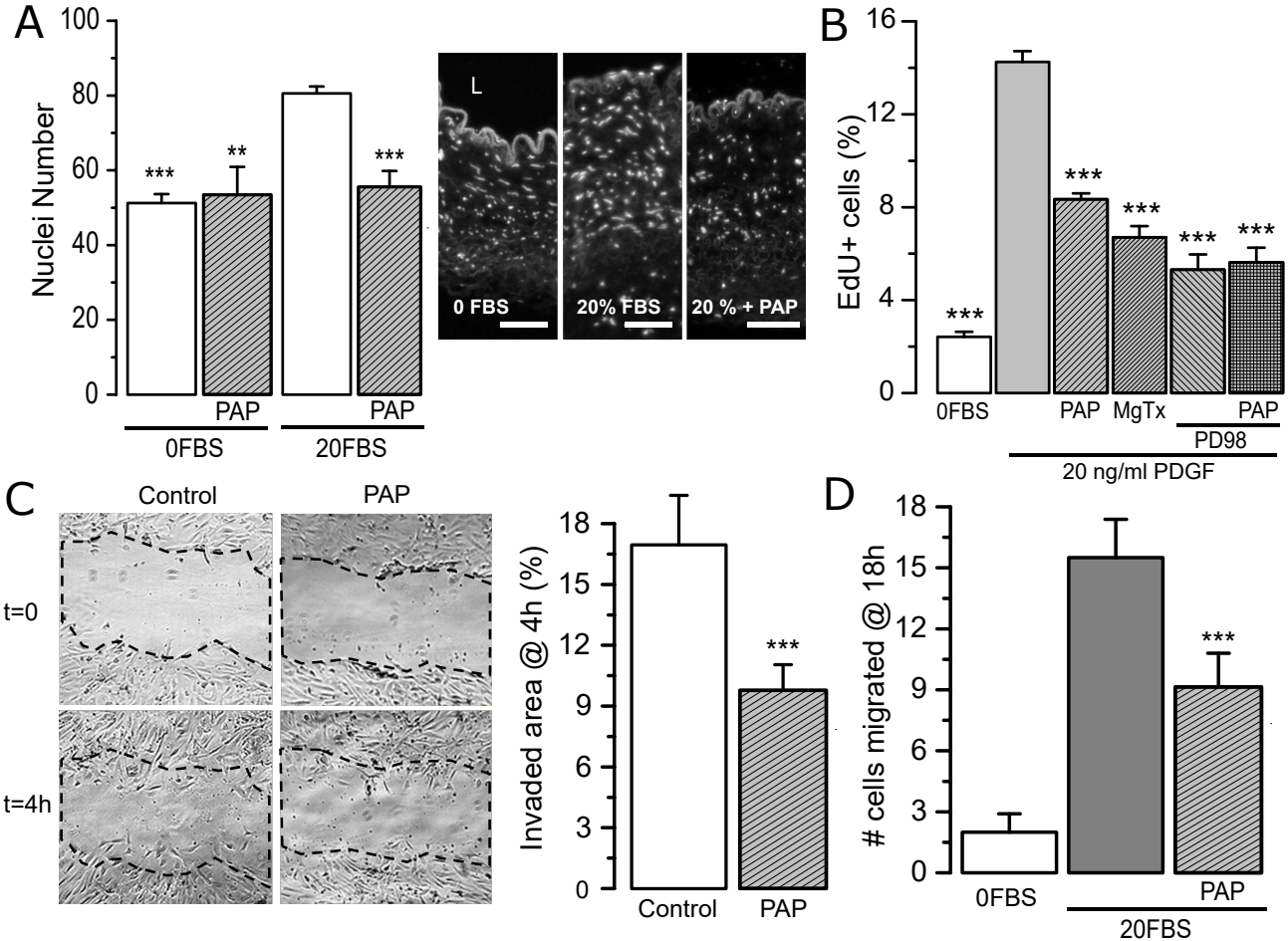
A
Nuclei Number
100
80
60
40
20
0
***
**
***
PAP
PAP
0FBS
20FBS
L
0 FBS
20% FBS
20 % + PAP
B
EdU+ cells (%)
16
12
8
4
0
***
***
***
***
***
0FBS
PAP
MgTx
PAP
PD98
20 ng/ml PDGF
C
Control
PAP
t=0
t=4h
Invaded area @ 4h (%)
18
15
12
9
6
3
0
***
Control
PAP
D
# cells migrated @ 18h
18
15
12
9
6
3
0
***
0FBS
PAP
20FBS

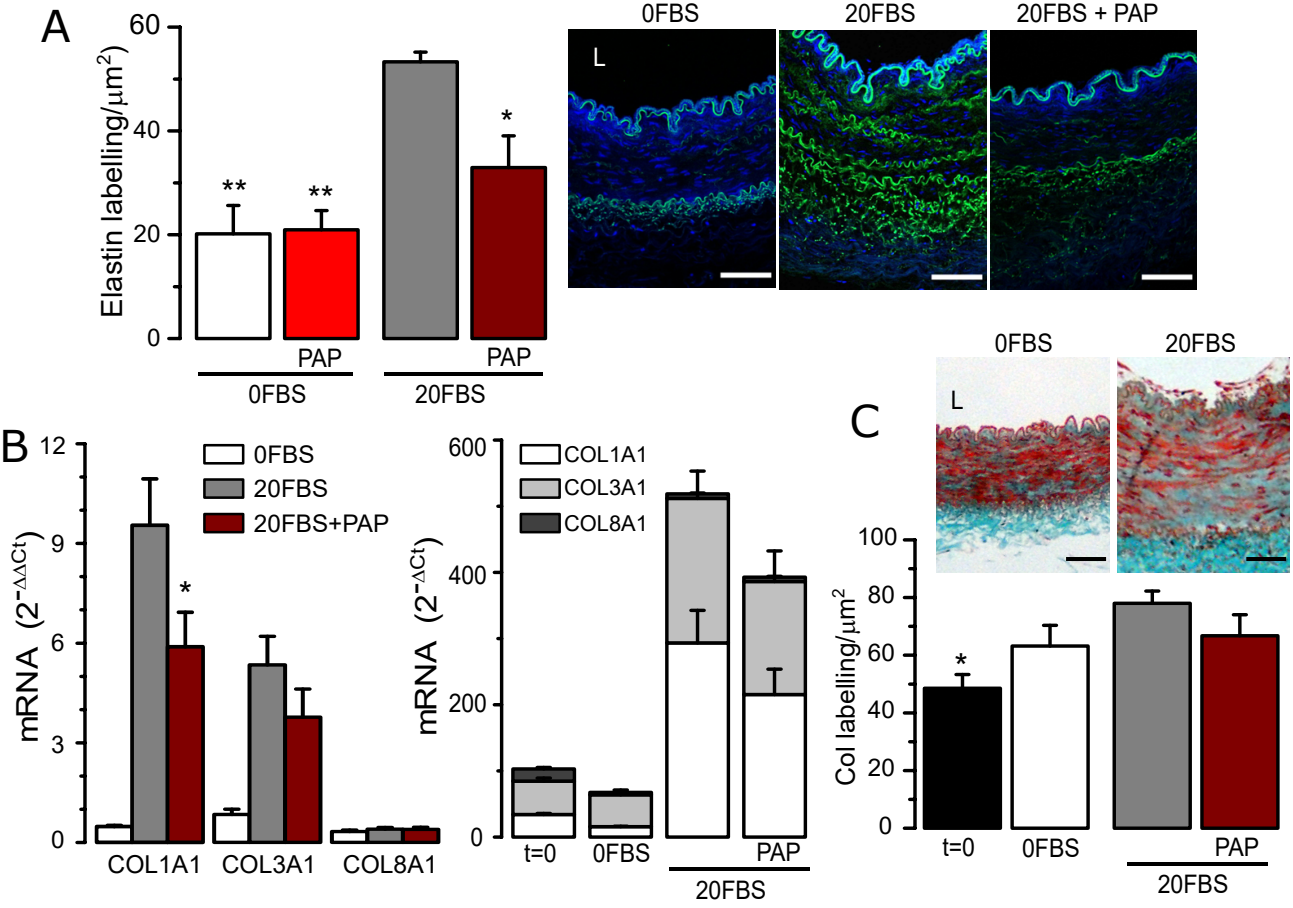
A
Elastin labelling/μm²
60
40
20
0
**
**
*
PAP
PAP
0FBS
20FBS
0FBS
20FBS
20FBS + PAP
L
B
mRNA (2^-ΔΔCt)
12
9
6
3
0
0FBS
20FBS
20FBS+PAP
*
COL1A1
COL3A1
COL8A1
mRNA (2^-ΔCt)
600
400
200
0
COL1A1
COL3A1
COL8A1
t=0
0FBS
PAP
20FBS
C
0FBS
20FBS
L
Col labelling/μm²
100
80
60
40
20
0
*
t=0
0FBS
PAP
20FBS

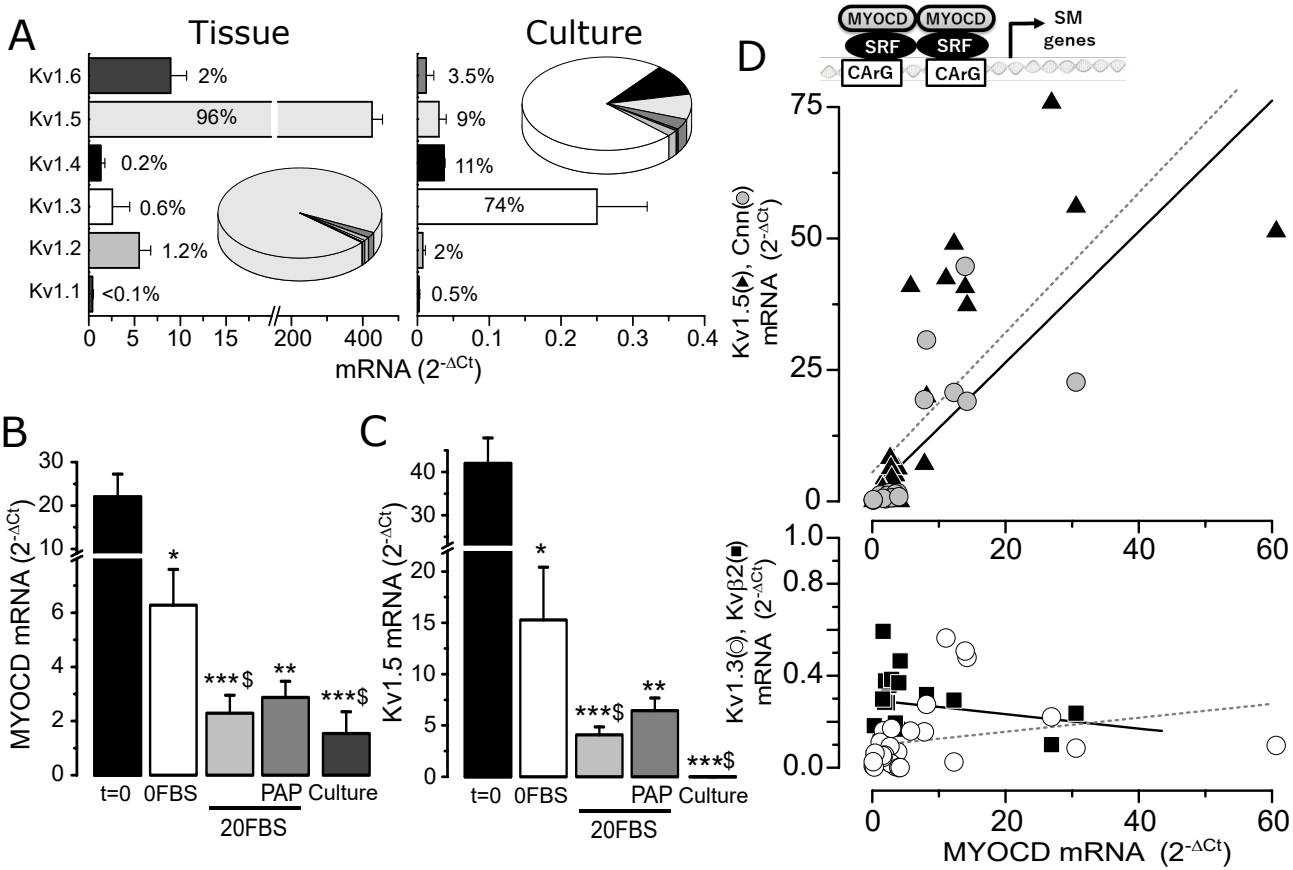
A
Tissue
Culture
Kv1.6
Kv1.5
Kv1.4
Kv1.3
Kv1.2
Kv1.1
2%
96%
0.2%
0.6%
1.2%
<0.1%
3.5%
9%
11%
74%
2%
0.5%
mRNA (2-ΔCt)
B
MYOCD mRNA (2-ΔCt)
t=0
0FBS
PAP
Culture
20FBS
C
Kv1.5 mRNA (2-ΔCt)
D
MYOCD
SRF
CArG
SM genes
Kv1.5(▶), Cnn(◎) mRNA (2-ΔCt)
Kv1.3(◎), Kvβ2(■) mRNA (2-ΔCt)
MYOCD mRNA (2-ΔCt)

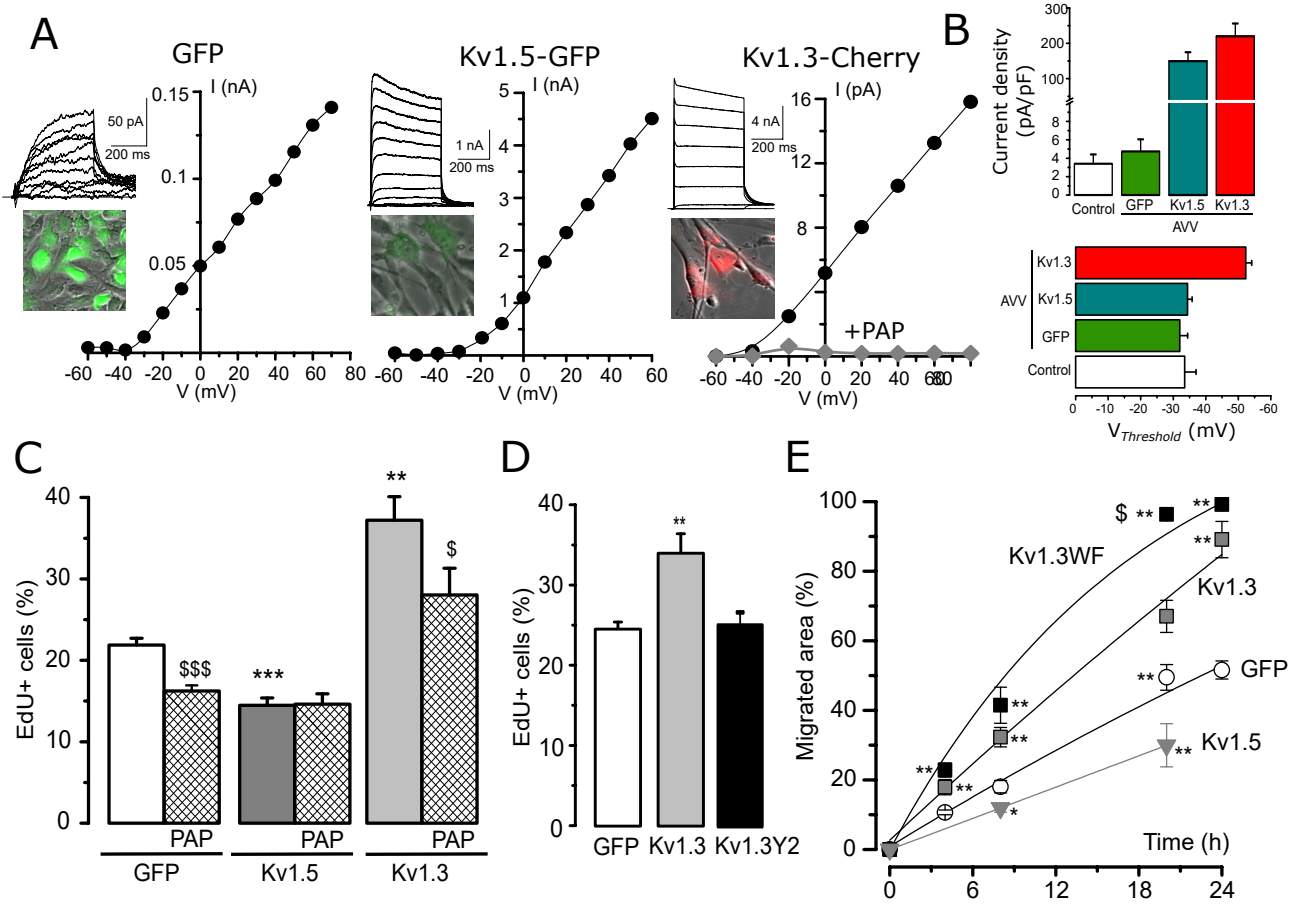
A
GFP
Kv1.5-GFP
Kv1.3-Cherry
50 pA
200 ms
1 nA
4 nA
I (nA)
I (pA)
V (mV)
+PAP
B
Current density (pA/pF)
Control
GFP
Kv1.5
Kv1.3
AVV
$V_{Threshold}$ (mV)
C
EdU+ cells (%)
PAP
$$$
***
**
$
GFP
Kv1.5
Kv1.3
D
EdU+ cells (%)
GFP
Kv1.3
Kv1.3Y2
E
Migrated area (%)
Kv1.3WF
Kv1.3
GFP
Kv1.5
Time (h)

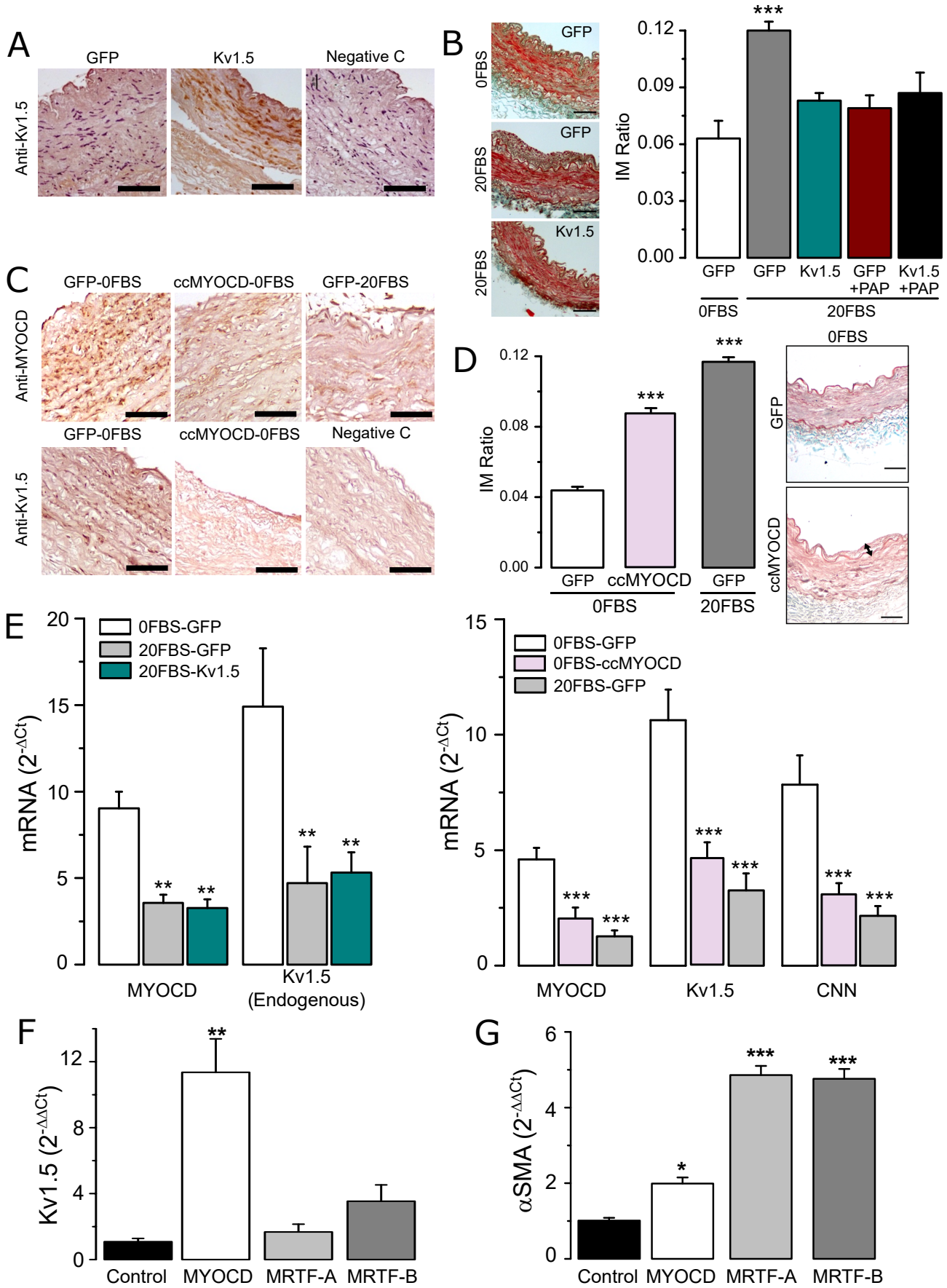
A
GFP
Kv1.5
Negative C
Anti-Kv1.5
B
0FBS
GFP
20FBS
GFP
20FBS
Kv1.5
IM Ratio
0.12
0.09
0.06
0.03
0.00
***
GFP
GFP
Kv1.5
GFP +PAP
Kv1.5 +PAP
0FBS
20FBS
C
GFP-0FBS
ccMYOCD-0FBS
GFP-20FBS
Anti-MYOCD
GFP-0FBS
ccMYOCD-0FBS
Negative C
Anti-Kv1.5
D
IM Ratio
0.12
0.08
0.04
0.00
***
***
GFP
ccMYOCD
GFP
0FBS
20FBS
0FBS
GFP
ccMYOCD
E
0FBS-GFP
20FBS-GFP
20FBS-Kv1.5
mRNA (2-ΔCt)
20
15
10
5
0
**
**
**
**
MYOCD
Kv1.5 (Endogenous)
0FBS-GFP
0FBS-ccMYOCD
20FBS-GFP
mRNA (2-ΔCt)
15
10
5
0
***
***
***
***
***
***
MYOCD
Kv1.5
CNN
F
Kv1.5 (2-ΔΔCt)
12
8
4
0
**
Control
MYOCD
MRTF-A
MRTF-B
G
αSMA (2-ΔΔCt)
6
4
2
0
*
***
***
Control
MYOCD
MRTF-A
MRTF-B

# SUPPLEMENTAL MATERIALS

**Myocardin-dependent Kv1.5 channel expression prevents phenotypic modulation of human vessels in organ culture.**

Marycarmen Arévalo-Martínez[1,2], Pilar Cidad[1,2], Nadia García-Mateo[1,2], Sara Moreno-Estar[1,2], Julia Serna[1,2], Mirella Fernández[5], Karl Swärd[6], María Simarro[3,2], Miguel A de la Fuente[4,2], José R López-López[1,2,] * and M Teresa Pérez-García[1,2,] *.

[1]Departamento de Bioquímica y Biología Molecular y Fisiología, [3]Departamento de Enfermería, [4]Departamento de Biología Celular, Universidad de Valladolid, [2]Instituto de Biología y Genética Molecular (IBGM), CSIC, [5]Cardiovascular Surgery Department, Hospital Clínico Universitario de Valladolid, Spain, [6]Department of Experimental Medical Science, University of Lund, Sweden.

# Supplemental Figures and Figure Legends

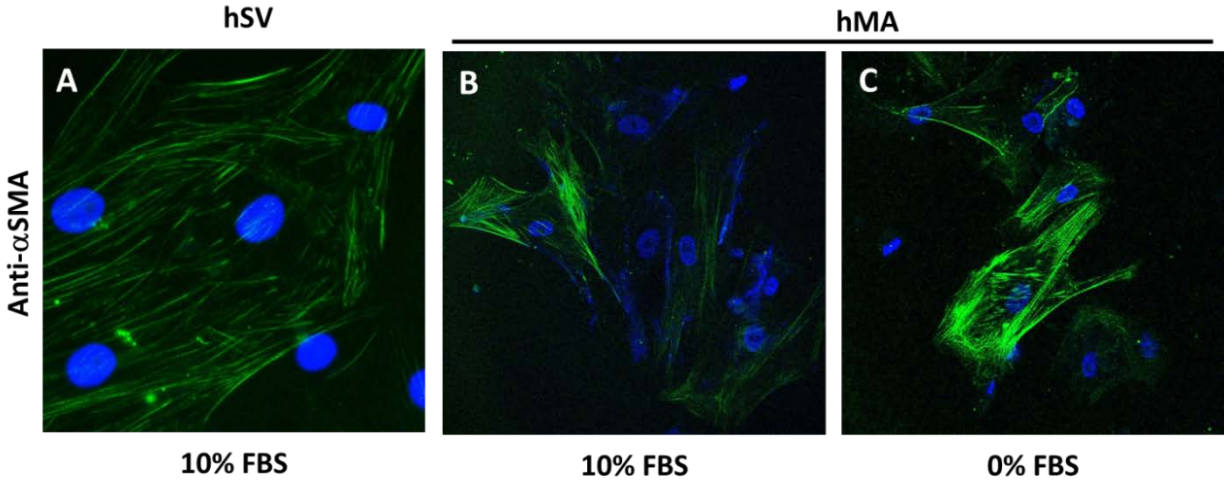


**Supplemental Figure I. Alpha Smooth Muscle Actin (αSMA) labelling in primary VSMC culture.** Representative microphotographs showing immunocytochemical labelling with αSMA antibody of primary VSMCs cultures at passage 7-8 obtained from human saphenous veins (hSV, **A**) and human mammary artery (hMA, **B** and **C**). While αSMA labelling was detected in most cells in hSV VSMCs even when they are kept in 10% FBS, in hMA expression of αSMA showed a weaker signal in these conditions (**B**) that could be increased upon treatment of the cells with serum free medium for 96h (**C**), a condition known to upregulate the expression of contractile proteins.

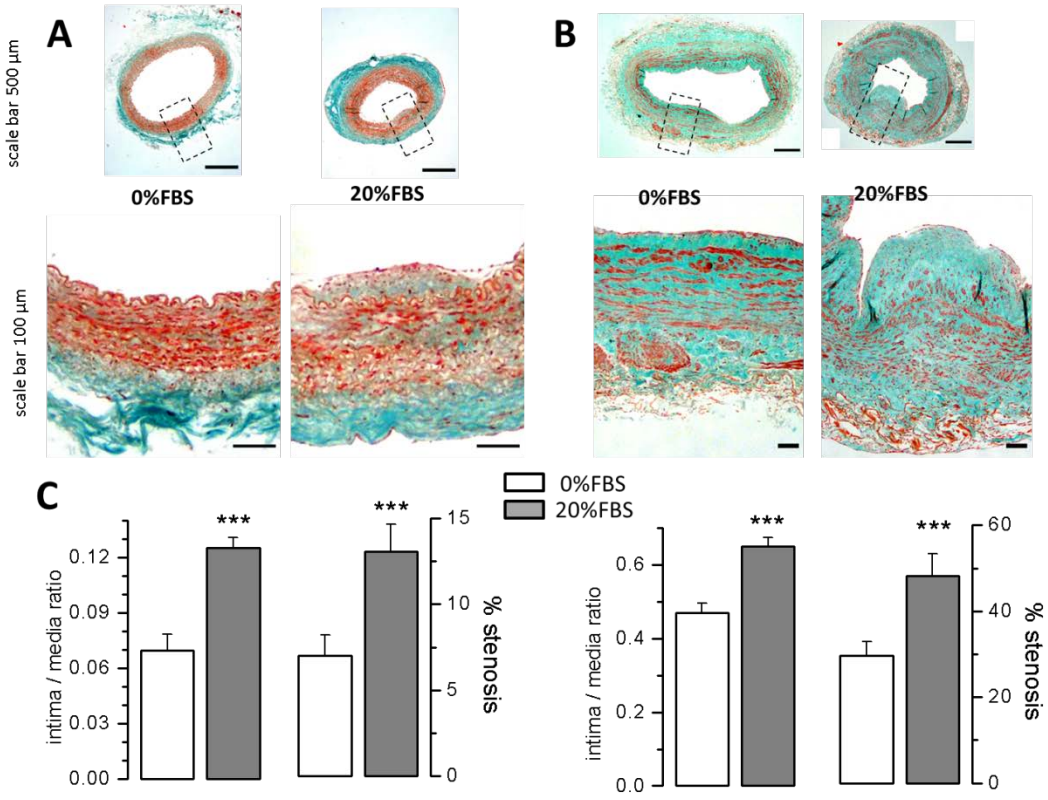


**Supplemental Figure II. FBS induces vascular remodeling after 2 weeks in organ culture. A and B**. Representative microphotographs of hMA (A) and hSV (B) stained with Masson trichrome after two weeks kept in organ cultured without (0%FBS) or with 20% FBS. The upper panels show images of the vessel rings (objective 4X, NA=0.13), and a section of the ring (indicated by the dotted square) is amplified in the lower panels, showing the presence of neointima (in hMA) or its increase (in hSV ) upon 20% FBS treatment. Scale bars= 500 µm (upper panels) and 100 µm (lower ones). L = lumen side. **C.** Vascular remodeling was quantified by determining the Intima/media ratio and % stenosis after two weeks in 0% FBS (white bars) or 20% FBS (gray bars). I/M ratio represents Intima area/Media area. Percentage of stenosis was calculated as : %stenosis = 100·(Intima area–Lumen area)/Intima area. Each bar is the Mean ± SEM of 18 hMA or 16 hSV. ***p<0.001 for paired data.

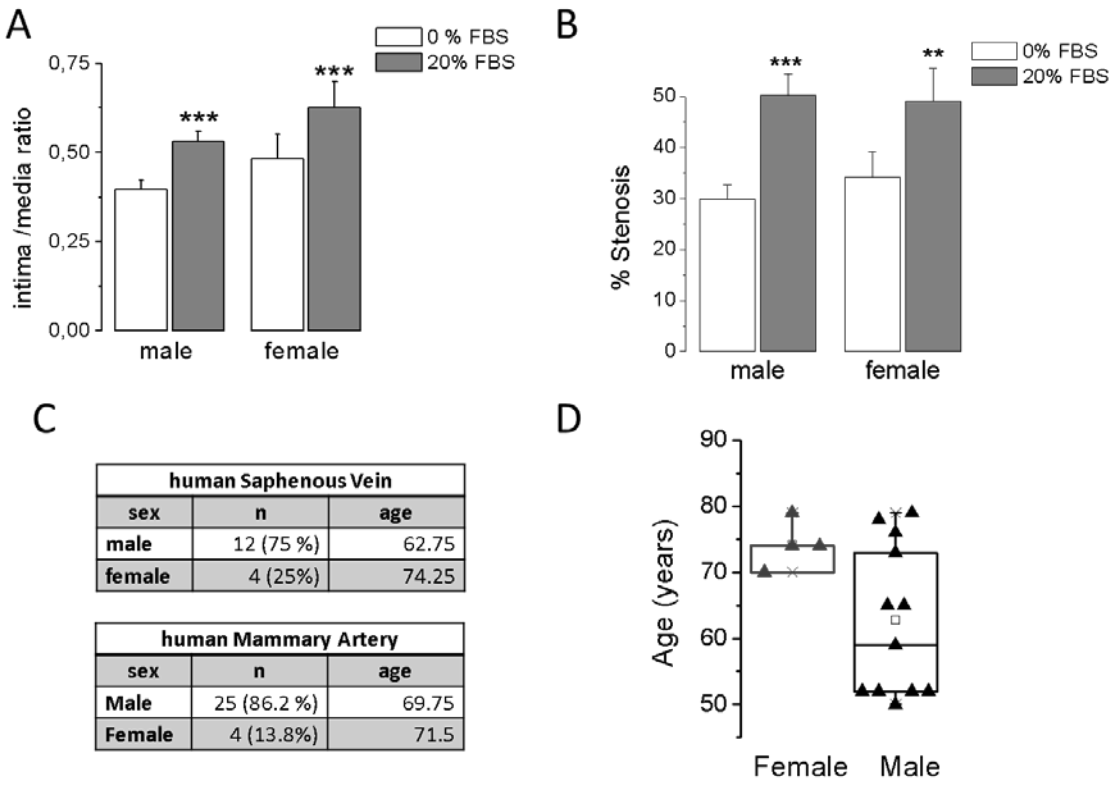


| human Saphenous Vein | | |
|---|---|---|
| **sex** | **n** | **age** |
| **male** | 12 (75 %) | 62.75 |
| **female** | 4 (25%) | 74.25 |

| human Mammary Artery | | |
|---|---|---|
| **sex** | **n** | **age** |
| **Male** | 25 (86.2 %) | 69.75 |
| **Female** | 4 (13.8%) | 71.5 |

**Supplemental Figure III. Organ culture of hSV does not have sex difference in the FBS- induced vascular remodeling**. **A** and **B.** Comparison of vascular remodeling in male and female hSV. The bar graphs show no differences in intima/media ratio (**A**) and % stenosis (**B**) between male and female samples. Data presented as Mean ± SEM, male n=12, female =4. ** p<0.01, ***p<0.001 as compared to 0%. **C**. Sex and age distribution (and percentages) of the mammary arteries and saphenous vein samples used in our study from which we could collect this information. **D**. Box plot showing the age distribution of the male and female hSV samples.

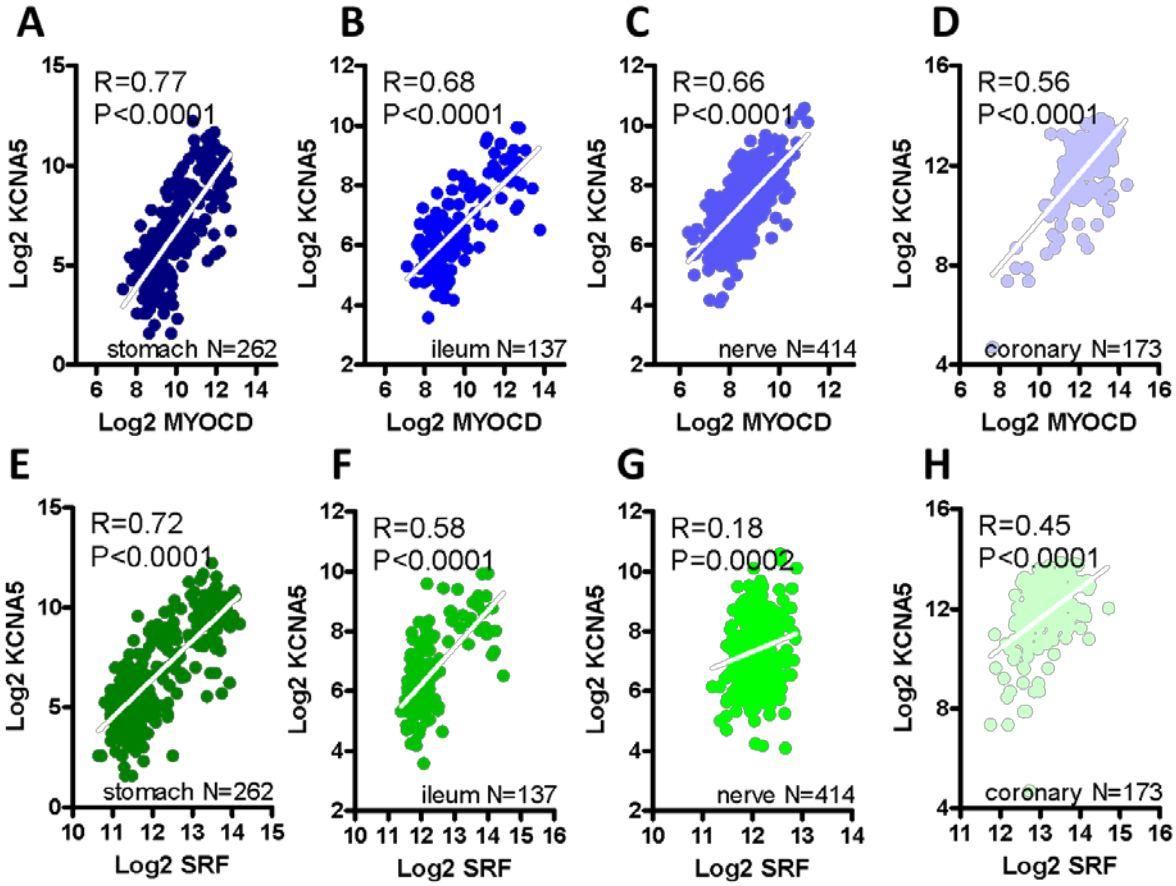


**Supplemental Figure IV. KCNA5 correlates with MYOCD and SRF at the mRNA level across human tissues.** RNA-Seq data was downloaded from the GTExPortal.org and normalized as described (Krawczyk KK, *et al.*, 2015). Correlations were tested in stomach (N=262), ileum (N=137), tibial nerve (N=414) and coronary artery (N=173) using Log2 transformed expression data and the Spearman method in GraphPad Prism. P-values, and Spearman Rho values are given in the panels (A through H). Straight white lines represent best linear fits.

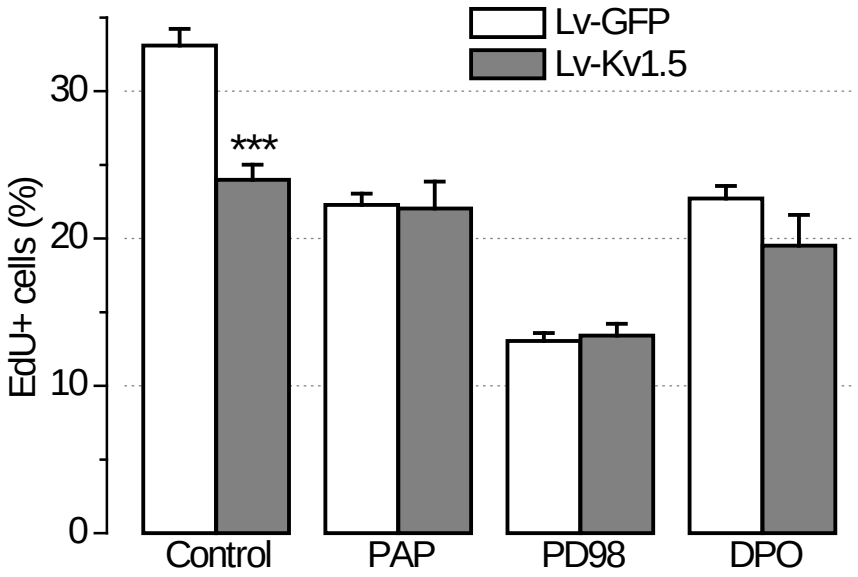


**Supplemental Figure V. Effect of Kv1.5 overexpression in VSMC proliferation.** Bar plot showing the proliferation rate of human coronary VSMCs infected with lentiviral vectors overexpressing GFP (white bars) or Kv1.5 (grey bars). Cells were incubated in control media alone or with 100 nM PAP-1 (PAP), 20µM PD98059 (PD98) or 2µM Diphenyl phosphine oxide-1 (DPO). All these treatments produced a significant decrease of proliferation in Lv-GFP cells, but only PD treatment inhibited Lv-Kv1.5 cells. Data presented as mean ± SEM, n=6-15 data from 3-6 different experiments. ***p<0.001 as compared to Lv-GFP.

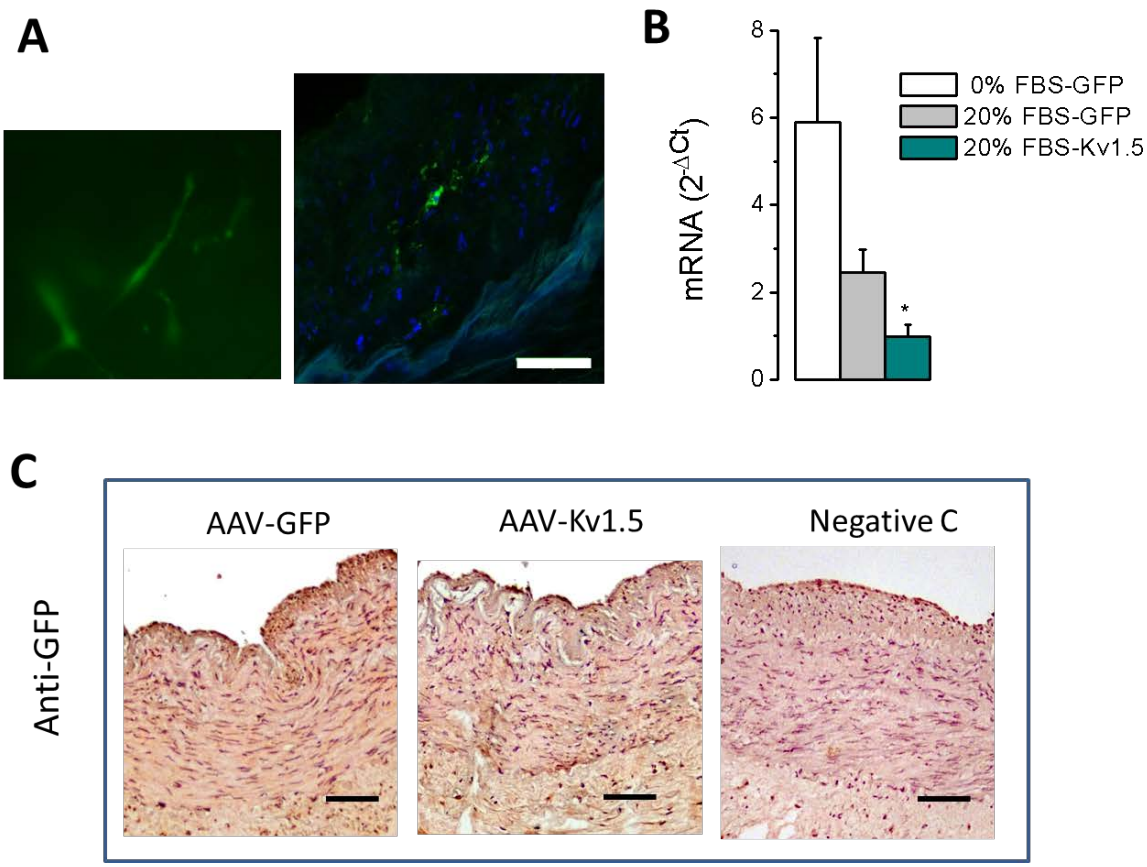


**Supplemental Figure VI. Control experiments to validate infection of hMA in organ culture with adenoviral vectors expressing GFP (control) or Kv1.5-GFP. A.** Microphotographs showing direct visualization of GFP-labelled cells form arterial rings in organ culture (upper image) or with confocal image of a paraffin section of hMA (lower image), nuclei labelled with Hoechst (blue) and scale bar = 50 µm. **B**. qPCR determination of the relative amount of GFP in hMA rings infected with AAV-GFP (kept in 0% or 20% FBS for two weeks) or with AAV-Kv1.5-GFP (kept in 20%FBS for two weeks). GFP mRNA was used as a control of infection, being absent from uninfected vessels. Data are Mean ± SEM of 4- 5 independent experiments. *p<0.05 compared to 0%FBS. **C.** Immunohistochemical labelling for GFP in paraffin-embedded cross-sections from hMA infected with AAV-GFP (left panel) or AAV-Kv1.5 (middle panel) and kept in organ culture with 20% FBS. Right panel show a negative control. 20X objective, scale bar = 100 µm.

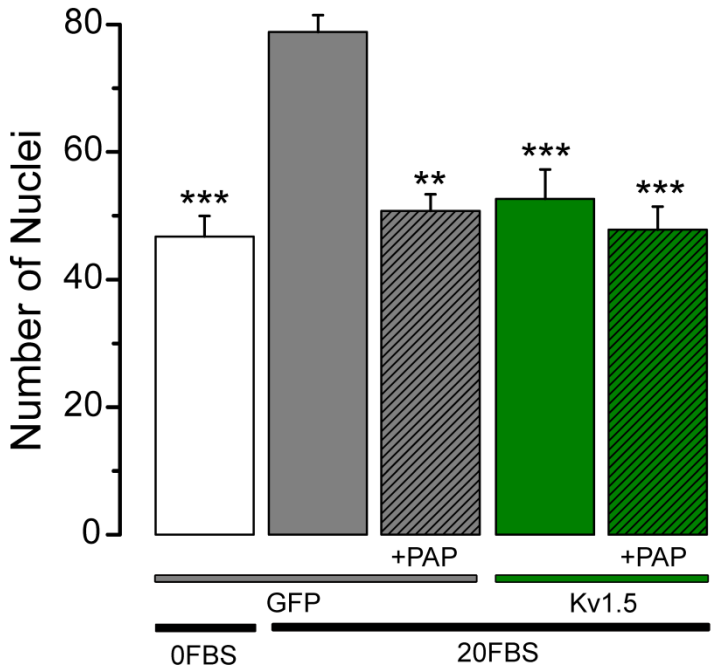


**Supplemental Figure VII. Characterization of the proliferation rate in AAV-Kv1.5-infected hMA rings in organ culture.** Proliferation rate was estimated by counting the nuclei present in the intima and media layer of hMA sections stained with Hoechst, as described in figure 2A. The experimental groups included control (AAV-GFP-infected samples, 0%FBS) and AAV-GFP-infected or AAV-Kv1.5-infected samples incubated with 20% FBS alone or in combination with PAP-1 (100nM) as indicated. Each bar is the mean ± SEM of 3-6 experiments. **p<0.01, ***p<0.001 compared to 20%FBS-GFP.

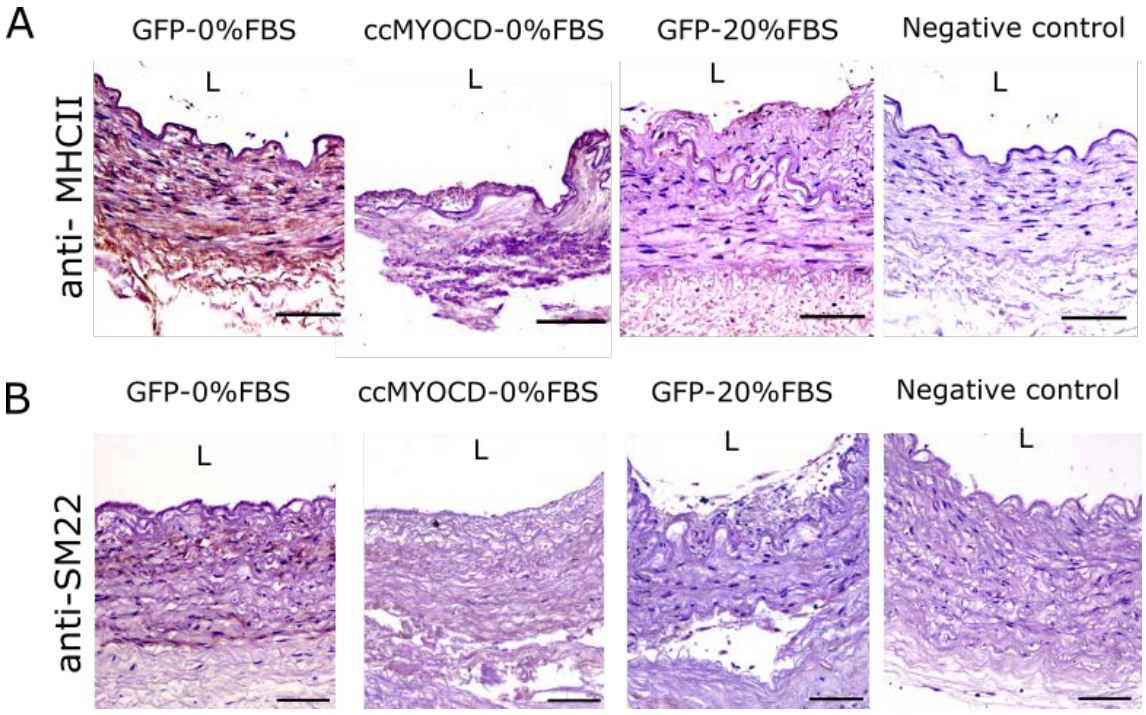


**Supplemental Figure VIII. Immunohistochemical characterization of the GFP and ccMYOCD-infected vessels in organ culture.** Representative microphotographs showing the labelling of the smooth muscle contractile proteins Myosin heavy chain II (MHCII, upper panels) and SM22 (lower panels) in paraffin-embedded cross-sections of hMA infected with Lv-GFP or the myocardin knock-down Lv-ccMYOCD. Arterial rings were kept in organ culture for 14 days in 0% or 20%FBS as indicated. MHCII and SM22 labelling can be clearly detected only in GFP infected cell kept in 0%FBS (left panels) and decreased significantly in the cc-MYOCD-0%FBS and GFP-20%FBS conditions. Right panels show the negative control for each antibody in a GFP-0% FBS sample. 10x objective (NA=0.3), scale bar 100µm. L = lumen side.

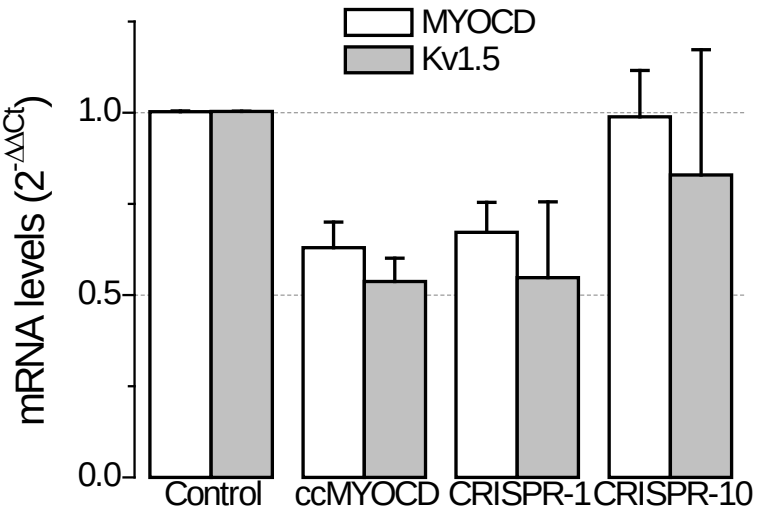


**Supplemental Figure IX. mRNA expression levels of Kv1.5 and Myocardin with the different myocardin knock-down vectors.** Myocardin knock-down experiments were carried out transducing hMA tissues with three different CRISPR/Cas9 vectors against Myocardin expression: CRISPR-1 (targeting exon 1), CRISPR-10 (targeting Exon 10), ccMYOCD (targeting both exons). Lv-GFP was used as control. Bar plot shows relative expression of MYOCD (white bars) and Kv1.5 (grey bars) using Lv-GFP as calibrator. The effects of ccMYOCD were reproduced with the CRISPR-1 while CRISPR-10 has no effect on myocardin and Kv1.5 mRNA expression.

| CRISPOR Scores | gRNA spacer myocardin Exon1 5'-GAACTTGCTCCTAATCAGCA-3' | gRNA spacer myocardin Exon 10 5'-GTGGTAGAAGCCGTTGGACA-3' |
|---|---|---|
| Specificity score | MIT- 79<br>CFD- 86 | MIT- 88<br>CFD- 93 |
| Efficiency score | 64 | 64 |
| Off-target mismatch counts | 0-0-1-11-123 | 0-0-1-8-75 |
| Most likely off-target | 0-0-0-0-1 | 0-0-1-0-0 |

**Supplemental Table I. CRISPOR scores for gRNAs targeting myocardin Exon1 and Exon10.** Table shows the CRISPOR scores obtained for gRNAs targeting myocardin used (http://crispor.org). Row 2 indicates two specificity scores: MIT (uses the formula from Crispr Website) and CDF (Cutting frequency determination, from guidescan.com) to predict how much an RNA guide sequence for a target may produce off-target cleavage. The scores range from 0-100, values over 50 are recommended. For the selected gRNAs both scores are higher than 50. The efficiency score (row 3), predicts how a target may be cut by its RNA guide sequence, it ranges from 0 to 100, and our efficiencies are higher than 50 for both gRNAs. Rows 4 and 5 show the number of possible off-targets in the genome for each number of mismatches (from 0 to 4 mismatches) and which are the most likely off-targets. There is one off-target with four mismatches for gRNA myocardin exon1 and also one with two mismatches for gRNA myocardin exon 10.

# Major Resources Tables

## Antibodies

| Target antigen | Vendor or Source | Catalog # | Working concentration | Lot # (preferred but not required) |
|---|---|---|---|---|
| Kv1.5 | Alomone | APC004 | 12 µg/ml | |
| GFP | NeuroMab | 75-131 | 20 µg/ml | |
| Myocardin | Sigma | SAB4200539 | 20 µg/ml | |
| Myosin Heavy Chain II | Abcam | AB683 | 20 µg/ml | |
| SM22 | Abcam | AB14106 | 8 µg/ml | |
| αSMA | Abcam | AB7817 | 4 µg/ml | |

## Target sequences (sgRNA) for myocardin knockdown

| Myocardin exon | sequence |
|---|---|
| Exon 1 | MYOCD EX1 FW: 5'-CACCGAACTTGCTCCTAATCAGCA -3'<br>MYOCD EX1 RE: 5'-AAACTGCTGATTAGGAGCAAGTTC-3'. |
| Exon 10 | MYOCD EX10 FW: 5'-CACCGTGGTAGAAGCCGTTGGACA-3'<br>MYOCD EX10 RE 5'-AAACTGTCCAACGGCTTCTACCAC-3'. |

## Taqman Assays

| gene | Protein | Assay ID (Thermo-Fisher) |
|---|---|---|
| KCNA3 | Kv1.3 | Hs00704943_s1 |
| KCNA5 | Kv1.5 | Hs00266898_S1 |
| CNN1 | Calponin | Hs00154543_m1 |
| MYOCD | Myocardin | Hs00538076_m1 |
| KCNAB2 | Kvβ2 | Hs01547935_m1 |
| COL1A1 | Collagen I | Hs00164004_m1 |
| COL3A1 | Collagen III | Hs00943809_m1 |
| COL8A1 | Collagen VIII | Hs00156669_m1 |
| HsRPL18 | Ribosomal protein L18 | F: 5'-aactgatgatgtgcgggttc-3', R: 5'-cagctggtcgaaagtgagg-3'<br>Probe: 5'-FAM-ctgaaggtatgtgcactgcgcgtga-BHQ2-3' |
| KCNA1 | Kv1.1 | Hs00264798_s1 |
| KCNA2 | Kv1.2 | Hs00270656_s1 |
| KCNA4 | Kv1.4 | Hs00937357_s1 |
| KCNA6 | Kv1.6 | Hs00266903_s1 |

## Cultured Cells (primary VSMCs from human mammary arteries)

| Name | Vendor or Source* | Sex (F, M) |
|---|---|---|
| 0013/384/02/0/01 | COLMAH collection (HERACLES network) | M |
| 0013/404/02/0/01 | COLMAH collection (HERACLES network) | M |
| 0013/407/02/0/01 | COLMAH collection (HERACLES network) | F |
| 0013/412/02/0/01 | COLMAH collection (HERACLES network) | M |
| 0013/386/02/0/01 | COLMAH collection (HERACLES network) | M |
| 0013/389/02/0/01 | COLMAH collection (HERACLES network) | M |
| 0013/368/02/0/01 | COLMAH collection (HERACLES network) | F |
| 0013/408/02/0/01 | COLMAH collection (HERACLES network) | M |

*(http:// www.redheracles.net/plataformas/en_coleccion-muestrasarteriales-humanas.html)

## Other Cultured Cells

| Name | Vendor or Source* | Sex (F, M) |
|---|---|---|
| hCASMCs | Gibco (Life Technologies, cat # 1130140) | Unknown |